LIFE HISTORY, ENVIRONMENT AND EXTINCTION OF THE SCALLOP *CAROLINAPECTEN EBOREUS* (CONRAD) IN THE PLIO-PLEISTOCENE OF THE US EASTERN SEABOARD

ANDREW L.A. JOHNSON,[1] ANNEMARIE M. VALENTINE,[1,2] MELANIE J. LENG,[3]
BERND R. SCHÖNE,[4] and HILARY J. SLOANE[3]

[1] *School of Environmental Sciences, University of Derby, Kedleston Road, Derby DE22 1GB, United Kingdom*
[2] *Current address: School of Geography and Environmental Science, Nottingham Trent University, Brackenhurst Campus, Southwell NG25 0QF, United Kingdom*
[3] *NERC Isotope Geoscience Facilities, British Geological Survey, Nicker Hill, Keyworth NG12 5GG, United Kingdom*
[4] *Institute of Geosciences, University of Mainz, Johann-Joachim-Becher-Weg 21, 55128 Mainz, Germany*
email: a.l.a.johnson@derby.ac.uk

RRH: TEMPERATURE VERSUS *PRIMARY PRODUCTION IN SCALLOP EXTINCTION*

LRH: A.L.A. JOHNSON ET AL.

ABSTRACT: **Plio-Pleistocene mass extinction of marine bivalves on the US eastern seaboard has been attributed to declines in temperature and primary production. We investigate the relationship of growth rate in the scallop *Carolinapecten eboreus* to variation in these parameters to determine which contributed to its extinction. We use ontogenetic profiles of shell $\delta^{18}O$ to estimate growth rate and seasonal temperature, microgrowth-increment data to validate $\delta^{18}O$-based figures for growth rate, and shell $\delta^{13}C$ to supplement assemblage evidence of production. Post-larval growth started in the spring/summer in individuals from the Middle Atlantic Coastal Plain but in the autumn/winter in some from the Gulf Coastal Plain. Growth rate typically declined with age and was usually higher in summer than winter. Many individuals died in winter but the largest forms typically died in spring, possibly on spawning for the first time. No individuals lived longer than two years and some grew exceedingly fast overall, up to 60% more rapidly than any other scallop species (< 145.7 mm in a year). Faster growth was generally achieved by secreting more rather than larger microgrowth increments. Some very fast-growing individuals lived in settings of high production and low temperature. No individuals grew slowly under high production whereas most if not all grew slowly under 'average' production and low temperature. In that the rapid growth evidently enabled by high production would have afforded protection from predators, Plio-Pleistocene decline in production was probably contributory to the extinction of *C. eboreus*. However, the negative impact of low temperature on growth under 'average' production suggests that temperature decline played some part.**

INTRODUCTION

During the Plio-Pleistocene, 45% of marine bivalve mollusk species became extinct in western Europe (Raffi et al. 1985), and 65% in the eastern US (Stanley 1986). The figure for the latter area includes a deduction for the rate of normal/background species loss, as estimated from relatively stable Plio-Pleistocene faunas in the western US and Japan, so species loss in the eastern US can truly be described as a mass extinction. High Plio-Pleistocene loss of marine mollusk species has been documented in the Caribbean area (Jackson et al. 1993; Jackson and Johnson 2000; Smith and Jackson 2009), so evidently an extinction event occurred throughout the North Atlantic region.

Bivalve extinction in the North Atlantic region was broadly coincident with the onset of northern hemisphere glaciation, and many warmth-favoring taxa were victims. Consequently, temperature decrease has been proposed as the cause (Stanley and Campbell 1981; Raffi et al. 1985; Stanley 1986; Stanley and Ruddiman 1995), with zones of upwelling cold water and (in the eastern US) increased seasonality invoked to explain the failure of warmth-adapted species to survive by migration southwards. An alternative (or supplementary) explanation in terms of a decline in primary production (food supply) has been suggested for the eastern US and Caribbean by Allmon and colleagues (Allmon et al. 1993, 1996; Allmon 2001), supported for the Caribbean by other workers (e.g., Todd et al. 2002), although a lagged response has been noted there (O'Dea et al. 2007). This lag might reflect localised persistence of high primary production (Leigh et al. 2014), indirect action of production decline through its effects on dominant habitat and hence predation intensity (Leonard-Pingel and Jackson 2016), or simply the time required for production decline (acting directly or indirectly) to bring about complete extinction (O'Dea and Jackson 2009; Smith and Jackson 2009).

As a contribution to debate over the cause of Plio-Pleistocene extinctions amongst marine bivalves in the eastern US, we present in this paper an investigation into the roles of declines in temperature and primary production in the extinction of a single species, the scallop (pectinid) *Carolinapecten eboreus* (Conrad, 1833). This species has a typical pectinid form but reaches an unusually large size (Fig. 1A), specimens up to 165 mm in height being known. Jones and Allmon (1995, fig. 10) obtained a long-wavelength ontogenetic profile of δ^{18}O from a large Florida Pliocene specimen. According to the standard interpretation of ontogenetic δ^{18}O profiles as signatures of seasonal temperature change, such long wavelength implies very rapid growth, which might have been a product of the high primary production indicated by other evidence (Allmon 1993; Allmon et al., 1995, 1996). We evaluate this possibility, and the question of whether decline in food supply rather than temperature led to the extinction of *C. eboreus*, through a wider investigation of growth rate in the species under circumstances of differing production and temperature. We use the associated fauna as an indicator of production and supply new estimates of temperature from shell δ^{18}O, also employing the seasonal fluctuation in this parameter as a time-marker to determine growth rate. We use shell δ^{13}C and the number and size of microgrowth increments (Fig. 1E, 1F) as supplementary indicators of production and growth rate, respectively.

Nearly 250 bivalve species were lost during the Plio-Pleistocene on the US eastern seaboard (Stanley 1986), so our results from one can only hint at the factor(s) affecting the rest. We hope, however, that our findings stimulate research on other species, and that the methodology we adopt (an application of sclerochronology) is seen as an approach worth repeating. Determining the cause of this recent mass extinction event is a worthwhile objective because of the potential for insights into the cause of other such events in the more distant past, and into the likely response of the current biota to environmental changes in the near future (e.g., global warming; Saupe et al. 2014a, b).

SCALLOP MODE OF LIFE, GROWTH RATE AND ENVIRONMENT: A FRAMEWORK FOR INVESTIGATING EXTINCTION

Most bivalves are suspension feeders and are benefited by morphological adaptations and/or life positions that confer stability, hence enabling uninterrupted acquisition of the small food particles concerned. A few scallops cement but most obtain stability by byssal attachment at small to medium sizes. Species growing to more than about 50 mm in height progressively abandon byssal attachment and become recliners (Brand 1991), obtaining stability through the weight of the shell. Additional thickening would be beneficial in this context, as well as a defence against crushing, drilling and prying predators, and has been used by a few forms (e.g., *Fortipecten*: Hayami and Hosoda 1988; Nakashima et al. 2004). However, the supplementary weight interferes with the alternative strategy towards predators available to scallops: escape through swimming. In many species, shell strength is increased without much addition of weight by plication (corrugation), thus preserving swimming ability to larger sizes. However, above about 70 mm, even the small weight increase associated with plication appears to be too much to permit swimming—at any rate, plicate scallops rarely swim above this size (e.g., Jenkins et al. 2003). By contrast, the non-plicate scallop *Placopecten* swims to a height of 100 mm (Dadswell and Weihs 1990), when differential increase in shell weight relative to the ability to provide forward propulsion and lift makes swimming mechanically impossible (Gould 1971). Beyond the height at which they are able to swim, scallops must adopt a 'siege' rather than 'flight' strategy towards predators, making use of the resistance to breakage, penetration and manipulation conferred by ontogenetic increase in shell thickness and by large size itself (Harper and Skelton 1993; Arsenault and Himmelman 1996; Harper et al. 2009). Numerous scallop species grow to a height at which they are immobile recliners so it would seem that a siege strategy towards predators is superior to flight (confirmed for *C. eboreus* by the absence of mollusk drillholes in the very many Plio-Pleistocene individuals above 80 mm height held by the Florida Museum of

Natural History, but presence in smaller scallops; Harper 2002; A.L.A. Johnson, personal observation, 2015). The rapid growth of many scallops (Bricelj and Shumway 1991, fig. 7) makes a siege strategy effective relatively early in life, and it is reasonable to surmise that any environmental circumstances favoring unusually rapid growth would be exploited for the benefits in relation to predation. Of the various factors affecting growth in bivalves, temperature and food supply are the most important in shelf settings of normal marine salinity, both in the group generally (Johnson et al. 2007; Moss et al. 2016, 2017; Abele et al. 2017) and scallops specifically (Bricelj and Shumway 1991; Thompson and Macdonald 1991). Evidence of unusually rapid growth can therefore be taken as a probable indication of relatively high temperature or primary production (the ultimate regulator of food supply to suspension-feeding bivalves, whether the particles ingested are living phytoplankton or organic detritus). Where one of these explanations is indicated independently, it can be presumed to be the cause of rapid growth.

In subsequent sections we describe temperature and primary production, as currently understood, in six time-space divisions of the Plio-Pleistocene sequence of the US eastern seaboard, predict variation in bivalve growth-rate amongst these divisions for models of temperature- and production-controlled growth, and then compare growth-rate results from *C. eboreus* with the predictions of each model. The environmental information supplied alongside growth-rate evidence by isotopic data from *C. eboreus* provides a significantly altered picture of temperature differences, and a slightly altered one of production differences, between the time-space divisions.

CAROLINAPECTEN EBOREUS: BACKGROUND INFORMATION AND MATERIAL INVESTIGATED

Forms that the authors of earlier systematic studies (Waller 1969; Gibson 1987) had referred to *Argopecten eboreus* (Conrad) were placed in the new genus *Carolinapecten* by Ward and Blackwelder (1987). The latter authors recognised only the species *C. eboreus*, but some authors (e.g., Petuch and Roberts 2007; Ward 2008; Waller 2018) have recognised others, although these species (like the various subspecies that have been recognised; Gibson 1987; Campbell 1993; Waller 2018) can be conceived as part of a single evolving lineage. This lineage, for which the name *C. eboreus* is used herein, arose in the Miocene and became extinct in the Pleistocene, having undergone little net phyletic change. Waller (1969) classed *C. eboreus* as an open-marine form. Other members of the *Argopecten gibbus* stock, from which he considered it to have evolved, were classed as bay scallops—i.e., inhabitants of semi-enclosed areas of sea, subject to fluctuations in salinity through fluvial discharge or evaporation.

The isotopic data from the Florida Pliocene *C. eboreus* specimen studied by Jones and Allmon (1995) was supplemented by Krantz (1990), who supplied δ^{18}O and δ^{13}C profiles from 12 Pliocene and Pleistocene *C. eboreus* specimens from Virginia and North Carolina. We have used these authors' isotopic results alongside our own (from 19 further specimens) to derive the fullest possible picture of variation in growth rate in relation to environment. Our strategy was to obtain an overview for the later part of the temporal range of *C. eboreus*, i.e., leading up to its extinction. We therefore ignored Miocene specimens and investigated individuals representing three broad time-intervals—'early Pliocene' (EPLI; essentially Zanclean: 5.3–3.6 Ma), 'late Pliocene' (LPLI; essentially Piacenzian: 3.6–2.6 Ma) and early Pleistocene (EPLE; Gelasian and Calabrian: 2.6–1.8 Ma)—from each of the Middle Atlantic Coastal Plain (MACP) and Gulf Coastal Plain (GCP). The data is weighted towards the LPLI and EPLE intervals (14 specimens from each) and includes some from the youngest formation containing *C. eboreus* in the GCP (Bermont Formation; Calabrian). At the time of data acquisition we thought that this was the youngest unit containing *C. eboreus* anywhere. However, we later discovered that the species occurs in the Flanner Beach and Canepatch formations of the MACP (Ward 2008), which are either of equivalent age to the Bermont Formation (Petuch and Roberts 2007) or from the middle Pleistocene (Ionian/Chibanian): ~ 0.5 Ma (Whitehead 1983; Ward 2008) or ~ 0.2 Ma (Miller 1985).

Note that we follow the recent revision of the geologic time scale (Gibbard et al. 2010), such that the Pliocene-Pleistocene boundary is at 2.6 Ma, with the Gelasian (formerly late Pliocene) now being the first stage in the Pleistocene. The 'mid-Pliocene' of previous authors (e.g., Dowsett et al. 2009; Williams et al. 2009; Winkelstern et al., 2103; Johnson et al. 2017) falls within the late Pliocene as defined above.

The specimens isotopically sampled by ourselves were either collected for the study (accessioned at the University of Derby: UD), or made available from existing collections at the Virginia Museum of Natural History (VMNH) and Florida Museum of Natural History (UF). To convey their time-space division, both the specimens sampled by ourselves and those sampled by Krantz (1990) and Jones and Allmon (1995) have been assigned new reference codes incorporating this information (Fig. 2). The specimens derive from the following units and locations (Fig. 3): EPLI-MACP—lower Yorktown Formation (Sunken Meadow Member) at Lee Creek Mine, Aurora, North Carolina (EPLI-MACP 1) and Claremont, Virginia (EPL1-MACP 2); EPLI-GCP—Unit 11 (Petuch 1982) at Sarasota, west-central Florida (EPLI-GCP 1, 2); LPLI-MACP—upper Yorktown Formation (Rushmere, Morgarts Beach and Moore House members) at Lee Creek Mine, Aurora, North Carolina and near/at Suffolk, Petersburg and Deep Creek, Virginia (respectively, LPLI-MACP 1, 2–6, 7, 8); LPLI-GCP—Tamiami Formation/Pinecrest Beds, Unit 2–10 (Petuch 1982), Sarasota County, west-central Florida (LPLI-GCP 1, 2, 4–6) and Jackson Bluff Formation, Leon County, north Florida (LPLI-GCP 3); EPLE-MACP—Chowan River Formation at Colerain

Beach, North Carolina (EPLE-MACP 1–7) and Deep Creek, Virginia (EPLE-MACP 8–10), and James City Formation at Lee Creek Mine, Aurora, North Carolina (EPLE-MACP 11, 12); EPLE-GCP—Caloosahatchee or Bermont Formation, Charlotte County, west-central Florida (EPLE-GCP 1) and Bermont Formation, Hillsborough County, west-central Florida (EPLE-GCP 2). More precise stratigraphic information (where available) is provided in Supplementary Data File 1, together with evidence of age. Despite uncertainties, possible ages show little overlap between specimens taken to represent different time intervals (EPLI, LPLI or EPLE; Fig. 2).

GROWTH-RATE PREDICTIONS FROM EXISTING EVIDENCE OF ENVIRONMENT

Extensive use has been made of biotic assemblages to interpret temperature and primary production in the Plio-Pleistocene of the US eastern seaboard, and substantial variation in both parameters has been recognised over the time-space divisions identified above (e.g., Hazel 1971, 1988; Ward et al. 1991; Cronin and Dowsett 1996; Allmon 1993, 2001; Allmon et al. 1995, 1996). Geochemical (mainly isotopic) approaches have added considerably to understanding of temperature variation (e.g., Krantz 1990; Roulier and Quin 1995; Jones and Allmon 1995; Goewert and Surge 2008; Tao and Grossman 2010; Winkelstern et al. 2013; Brachert et al., 2014; Johnson et al. 2017) but so far have only been used a little to investigate production (Krantz 1990; Jones and Allmon 1995; Tao and Grossman 2010), with a focus on determining the cause of variation. In the next sections, we use existing isotopic (δ^{18}O) temperature data from mollusks (where available) in combination with qualitative assessments of production from faunal composition to characterise the environment of each division. We thus identify which divisions should yield evidence of rapid growth if temperature or production was the controlling factor. Isotopic temperature data of a similar (seasonal) resolution to that from mollusks has been obtained from corals (e.g., Roulier and Quinn 1995) but there are discrepancies between the two datasets—e.g., systematically lower seasonal temperature variation indicated by corals (Brachert et al. 2014). Combining the datasets would have obscured differences between the divisions.

Temperature

With the exception of information from the lower James City Formation of the early Pleistocene (Krantz 1990), Johnson et al. (2017) summarised all the available molluscan $\delta^{18}O$ data (entirely from bivalves) for the early Pliocene to early Pleistocene of the MACP, giving temperatures calculated for appropriate values of water $\delta^{18}O$. Winter minimum and summer maximum temperatures for specific units and taxa (including already-analysed *Carolinapecten*) are listed in Table 1. Temperatures for the lower James City Formation, calculated on the same basis as those for the early Pleistocene Chowan River Formation (i.e., water $\delta^{18}O$ = 0.00‰) have been added. Table 1 shows that material of LPLI age gives higher winter and summer temperatures than material of EPLI and EPLE age. We can conveniently define high temperature conditions (represented by LPLI data) and differentiate these from low temperature conditions (represented by EPLI and EPLE data) by setting winter and summer boundaries of 11.5 °C and 24 °C, respectively, between the two.

Applying the classification scheme adopted for the MACP to the GCP, gastropod-derived data from Unit 7 of the Pinecrest Beds (LPLI) clearly falls within the high temperature category: mean winter and summer isotopic temperatures calculated using an appropriate value (+1.02‰) for water $\delta^{18}O$ are 18 and 27 °C, respectively (Tao and Grossman 2010, table 1). On the basis of Sr/Ca data, Tao and Grossman (2010) argued that their lower gastropod-derived isotopic temperatures from Unit 4 (also LPLI) reflected inappropriate use of the same value for water $\delta^{18}O$. A higher value (reflecting likely evaporative enrichment of ^{18}O in seawater during deposition of this unit) would have yielded correspondingly higher temperatures. Earlier gastropod and bivalve $\delta^{18}O$ data from other LPLI (and EPLE) units within the Pinecrest Beds (Jones and Allmon 1995) yields temperatures generally similar to the more recent gastropod data from Unit 7 when calculated using a water $\delta^{18}O$ of +1.02‰ (Tao and Grossman 2010, figure 4). Use of this value for gastropod $\delta^{18}O$ data from the Caloosahatchee Formation (EPLE) yields mean winter and summer temperatures of 17 and 27 °C, respectively (Tao and Grossman 2010, table 1). However, we prefer (see below) a value of 0.00‰ for the EPLE interval, which yields temperatures 4–5 °C lower, within the high temperature category as defined above for winter but outside it for summer. We therefore recognise an additional low summer (LS; < 24 °C)/high winter (HW; ≥ 11.5 °C) temperature category. This category appears to be represented not only by the EPLE-GCP but also the EPLI-GCP division. No isotopic temperature data has been provided hitherto for the latter but ostracod-assemblage analysis gives mean winter and summer temperatures (16 and 22 °C, respectively; Cronin and Dowsett 1996) that fall within the LS/HW category. Isotopic evidence from the MACP indicates that ostracod-assemblage analysis may yield winter temperatures that are overestimated by 3–4 °C (Johnson et al. 2017). However, subtraction of this amount from the assemblage-derived EPLI-GCP winter value still leaves a figure in the high temperature range. In view of the refinement to the classification scheme necessitated by EPLI-GCP and EPLE-GCP data it is appropriate also to recognise a high summer (HS; ≥ 24 °C)/low winter (LW; < 11.5 °C) temperature category, not represented by existing data from the early Pliocene to early Pleistocene of the US eastern seaboard, but into which new data might fall.

Primary production

The Miocene of the US eastern seaboard is characterised by thick phosphorite deposits, almost certainly reflecting high primary production, i.e., a supply of organic material too large for respiration to prevent its accumulation on the seafloor (Riggs 1984; Riggs et al. 2000; Snyder et al. 1990). Phosphate is also present in many Pliocene and early Pleistocene units, and occurs in amounts up to 25% in the EPLI interval (Riggs et al., 1982), but was probably derived from erosion of Miocene phosphorites rather than generated contemporaneously (Riggs et al. 2000; S.R. Riggs, personal communication, 2016). Nevertheless, compelling evidence of high production exists for some Pliocene units in the form of rich marine vertebrate faunas, including numerous fish-eating birds and other predators, some of large size. The occurrence of common turritelline gastropods has been used as an indication of high production (e.g., Allmon 2011; Allmon et al. 1995; Anderson et al. 2017). However, in some situations high frequencies reflect cool water rather than high production (Allmon and Dockery 1992) so to avoid ambiguity we limit the following discussion to vertebrate evidence. Existing geochemical evidence of production is too scant to permit comparison between divisions by this means.

The Pliocene Yorktown Formation of Lee Creek Mine, Aurora, North Carolina, has yielded an abundant and diverse fauna of marine fish (Fierstine 2001; Purdy et al. 2001), including the giant shark *Carcharocles megalodon*, together with diverse, sometimes large, carnivorous marine mammals (Kohno and Ray 2008; Koretsky and Ray 2008; Whitmore and Barnes 2008; Whitmore and Kaltenbach 2008; Kazár and Bohaska 2008), and an abundant avifauna consisting of over 100 species, mostly marine fish-eating forms (Olson and Rasmussen, 2001; Storer 2001; Olson and Hearty 2003). Virtually all the many thousands of vertebrate specimens are from spoil but characteristics of the attached matrix allowed the above authors to assign much of the material to the lower part of the formation, i.e., the

Sunken Meadow Member (EPLI-MACP). While noting that some vertebrate material is from higher horizons (thus ruling out exceptional preservational circumstances in the lower Yorktown Formation), Ward (2008) agreed that most came from the Sunken Meadow Member, remarking (p. 360) in a summary of the biota of the overlying Rushmere and Morgarts Beach members (LPLI-MACP) that the ‘relative lack of vertebrates is especially noticeable.’ The same pattern is evident elsewhere in the MACP. For instance, Kohno and Ray (2008) list numerous EPLI occurrences of walruses but just one definite LPLI record (Appendix II, number 4; a locality in Virginia exposing only the upper Yorktown Formation according to Ward and Blackwelder 1980); similarly, there is just a single LPLI record of a whale and of a seal, both from Rice’s Pit, Hampton, Virginia (Westgate and Whitmore 2002; Koretsky and Ray 2008, p. 114). Ward (2008) recorded no vertebrates at all from the uppermost (Moore House) member of the Yorktown Formation or from the early Pleistocene Chowan River Formation at Lee Creek, but a walrus femur from Yadkin Pit, Deep Creek, Virginia, may be from the latter unit, even if probably reworked from the Yorktown Formation (Kohno and Ray 2008, Appendix 1; Appendix 2, number 5). The depauperate nature of the EPLE-MACP vertebrate fauna is also evident in the younger James City Formation at Lee Creek, from which Ward (2008) listed only a restricted fish assemblage (four species), commenting (p. 384) that the ‘scarcity of shark, ray and bony fish remains in units above the Sunken Meadow Member of the Yorktown Formation (lower Pliocene) is reflected in all of the stratigraphic units along the Atlantic Coastal Plain. The James City Formation is typical in this regard.’ Certainly the still younger Flanner Beach Formation is no exception: Ward (2008) lists no vertebrates from this at Lee Creek.

On the basis of the abundance, diversity and ecology of vertebrates from Lee Creek, Olson and Rasmussen (2001, p. 238) opined: ‘The Yorktown seas off present-day North Carolina must have supported one of the greatest levels of marine productivity in the history of the earth.' In that most of the Yorktown marine vertebrate fauna (here and elsewhere in the MACP) is from the Sunken Meadow Member, this statement can be taken to apply to the EPLI interval, with much lower production in the LPLI and EPLE intervals in the MACP, probably at something like the 'average' shelf level characteristic of the US eastern seaboard at present (FAO 1981, map 1.1).

While it lacks birds and has a fish fauna apparently limited to sharks (Petuch and Roberts 2007), the vertebrate fauna of Unit 1 of the Sarasota, Florida, sequence (EPLI-GCP) includes abundant and diverse carnivorous marine mammals, some of large size (Emslie and Morgan 1994; Allmon et al. 1996), and thus resembles that of the Sunken Meadow Member. Similarly high production can therefore be inferred. Unlike in the MACP, high production evidently continued (or at least recurred) in the LPLI interval in the GCP. A bed at the Richardson Road Shell Mine (= Quality Aggregates pit), Sarasota, that is contemporaneous with or somewhat older than Unit 4 (Allmon 1993), contains an avifauna of 11 taxa, with one extinct, probably marine, cormorant species represented by 137 skeletons and thousands of separate bones (Emslie and Morgan 1994; Emslie et al. 1996). No fully marine cormorants live in Florida now so the occurrence of such a form in large numbers during the LPLI interval provides good evidence of more abundant food than at present in the shape of marine fish, and thus of higher primary production (Allmon et al. 1996). By the EPLE interval production had seemingly declined in the GCP to something like the present 'average' level (FAO 1981, map 1.1): two seabird species (an alcid and an albatross; both known from single bones) are recorded from the Caloosahatchee Formation and a seal from the Bermont Formation, suggesting a fairly limited marine bird and mammal fauna, similar to that at present in Florida and contrasting sharply with the Pliocene (Allmon et al. 1996).

Growth-rate predictions

On the basis of present evidence, nearly all possible combinations of the temperature and production categories identified above are represented by time-space divisions in the Plio-Pleistocene of the US eastern seaboard (Fig. 4). We can expect there to have been a temperature and level of production above which growth in *C. eboreus* was inhibited rather than promoted. Tests of the influence of each parameter on growth are therefore best framed in terms of predictions relating to relatively low values of each. Thus if temperature was the control we should not expect to see rapid growth in settings of low winter and summer temperature (in the EPLI-MACP and EPLE-MACP divisions from present evidence); if production was the control we should not expect to see rapid growth in settings of 'average' production (in the LPLI-MACP, EPLE-MACP and EPLE-GCP divisions from present evidence); and if both were involved we should not expect to see rapid growth in settings of low winter and summer temperature combined with 'average' production (in the EPLE-MACP division from present evidence).

LABORATORY METHODS AND TREATMENT OF DATA

As indicated above, we used the isotopic data of Krantz (1990) and Jones and Allmon (1995) to supplement our own from *C. eboreus*. The specimen investigated by Jones and Allmon (1995) was available, so we obtained complementary microgrowth-increment data from it. The specimens analysed by us were (where necessary) initially scrubbed with a nylon brush in tap-water to remove loosely adherent sediment. They were then coated with a sublimate of NH_4Cl and digitally photographed. Images were inserted into the bespoke software Panopea© (2004, Peinl and Schöne) for counting and measurement of microgrowth increments, together with measurement of the position of significant growth breaks, subdivided into major and moderate according to the size of the 'step' in the shell profile (Fig. 1A, 1C, 1F). In all shells the lamellae bounding microgrowth increments had been affected by abrasion near the dorsal margin (umbonal area), preventing acquisition of complete microgrowth-increment records, and visibility was sometimes poor elsewhere. Measurements of increment sizes and growth-break positions were made principally along the mid-line (axis of maximum growth = anatomical height) but for most shells it was preferable (e.g., to avoid areas of abrasion), and for two broken shells (e.g., Fig. 1C) necessary, to include measurements taken somewhat anterior or posterior of this line. In such instances increment sizes and growth-break 'heights' were mathematically adjusted (multiplied by umbo–margin distance along mid-line/umbo–margin distance through measurement position) to correspond to measurements along the mid-line. The same adjustment was made to the measured position of isotope samples where these were taken away from the mid-line—e.g., in cases of breakage or other shell imperfections (see below).

Following removal of the NH_4Cl coating by washing in tap-water, specimens for isotopic analysis were thoroughly cleaned using the method adopted by Valentine et al. (2011). Samples were extracted by drilling successive, continuous or discontinuous (plical crests only) grooves up to about 1 mm deep in the outer shell layer (foliated calcite apart from a short prismatic-calcite stage in the right valve; Waller 1978), using a hand-held drill equipped with a 0.5 mm bit. The spacing of grooves was varied according to microgrowth-increment size (and hence presumed growth rate) to achieve roughly comparable temporal resolution within and between specimens: mean spacings for individuals (as determined for the axis of maximum growth) are 1.5–4.7 mm. Cracks and areas significantly abraded or with a high concentration of microborings were avoided. In a few instances, encrusting organisms or sediment were drilled away to reveal the shell; the outermost part of the shell itself (~ 0.1 mm) was also drilled away in a few cases where it had an unusual colour or texture. Where practicable, sampling was started very close to the dorsal margin (origin of growth) and continued to the ventral margin, but in some cases breakage or abrasion had reduced the already small amount of material recoverable close to the dorsal margin to such an extent that sampling had to commence more ventrally. It was noted in sampling close to the dorsal margin that material of a different (often 'crystalline') character to that of the (there thin) outer shell layer was sometimes revealed and possibly included in the material extracted. Samples were removed from the site of extraction by partially or wholly inverting the shell such that, with the assistance of tapping or brushing, the powder fell onto a slip of aluminium foil for collection and transfer into a non-stick storage vial. After extraction and removal of each sample the shell was thoroughly brushed to prevent contamination of the next sample.

Measurement of $\delta^{18}O$ and $\delta^{13}C$ was carried out either at the NERC Isotope Geosciences Laboratory, British Geological Survey, Keyworth, UK, or at the Institute of Geosciences, University of Mainz, Germany. Analysis at Keyworth involved an Isoprime dual inlet mass spectrometer coupled to a Multiprep system; powder samples were dissolved with concentrated phosphoric acid in borosilicate Wheaton vials at 90 °C. Analysis at Mainz involved a Thermo Finnigan MAT 253 continuous flow-isotope ratio mass spectrometer coupled to a Gasbench II; powder samples were dissolved with water-free phosphoric acid in helium-flushed borosilicate exetainers at 72 °C. Both laboratories calculated $\delta^{18}O$ and $\delta^{13}C$ against VPDB and calibrated data against NBS-19 and their own Carrara Marble standard; values were consistently within ± 0.05‰ of the preferred values for $\delta^{18}O$ and $\delta^{13}C$ in NBS-19. For a few shells, part of the sample series was analysed in one laboratory and part in the other; there was found to be excellent agreement (e.g., smooth continuation of trends) between the subsets of data. Reproducibility was checked by remeasuring some samples, and in the case of seemingly aberrant initial results, repeat sampling and analysis was undertaken (both initial and replicate values are plotted in Figs. 5–8). Results from repeat sampling were nearly always closer to expectation (implying some contamination of the initial samples) and in such cases were used with singleton values from other positions to generate ontogenetic profiles (lines in Figs. 5–8). Otherwise, the profiles connect singleton values with mean values from multiple sampling (and multiple measurement). Figure 6A contains the isotopic results of Jones and Allmon (1995; read off from fig. 10).

To conform with recent work on Plio-Pleistocene scallops from the US eastern seaboard (Johnson et al., 2017), temperatures were derived from shell $\delta^{18}O$ using the calcite equation (1) of Epstein et al. (1953):

$$T = 16.5 - 4.3(\delta^{18}O_{calcite} - \delta^{18}O_{seawater}) + 0.14(\delta^{18}O_{calcite} - \delta^{18}O_{seawater})^2 \qquad (1)$$

We subtracted 0.27‰ from our $\delta^{18}O$ water values (calibrated against SMOW) in order to adjust them to the VPDB scale used for shell carbonate (Gonfiantini et al. 1995). Various initial values for water $\delta^{18}O$ were used. Whilst noting that global, negative estimates have been adopted by some workers (discussed in Johnson et al. 2017), we favor the model-based, regional, positive estimates for the Pliocene given by Williams et al. (2009): +0.70 and +0.90‰ for the early Pliocene of the MACP and GCP, respectively; +1.10 and +1.02‰ for the late Pliocene of the MACP and GCP, respectively. We calculated temperatures from each Pliocene $\delta^{18}O$ profile using all four estimates of water $\delta^{18}O$ but prefer those based on the relevant division-specific value. Model-based regional estimates of water $\delta^{18}O$ do not exist for the early Pleistocene of the US eastern seaboard so we used the set of four estimates (–0.20, 0.00, +0.20, +0.50‰) employed by Winkelstern et al. (2013) for this interval, following these authors in adopting 0.00‰ as the preferred value.

Notwithstanding the existence of some 'noise', the summer (low values) and winter (high values) parts of $\delta^{18}O$ profiles were in general readily identifiable (problematic cases are discussed in the next section). In accordance with the approach of Johnson et al. (2017), we used the maxima and minima of unsmoothed profiles to derive values for extreme winter and summer temperatures. The shell heights of maxima and minima were likewise used to determine the size of half- and (in most cases) whole-year shell increments—i.e., growth rate. As for estimation of seasonal temperature, the use of maxima and minima from unsmoothed δ^{18}O profiles to determine the size of half- and whole-year increments introduces the possibility of error relating to noise. However, smoothing has some disadvantages (e.g., amplification of the effect of growth breaks; Johnson et al. 2017) and is not a solution to errors of a more systematic nature (see discussion of early ontogenetic excursions below). As will be shown, *C. eboreus* had a very short lifespan (never exceeding two years and rarely much more than one) so only a modest proportion of the δ^{18}O profiles (9 of 32) contain two maxima and/or minima, others showing one maximum and one minimum or a single maximum/minimum (partly due to incomplete or inadequate shell preservation). In cases of the last two types it was only possible to obtain minimum values for whole- and half-year increments, respectively. We determined the largest half- and (for individuals that lived sufficiently long) whole-year increment from each profile, measuring the size of the largest whole-year increment between consecutive δ^{18}O maxima or minima, or between other homologous points (i.e., δ^{18}O values representing equivalent times of year) where this gave a larger value. The approach is illustrated in Figures 5–8, where we have identified the points on the δ^{18}O profiles between which half-year and whole-year increments were measured (see also Fig. 1A–C). The same methodology was followed in measurement of increment sizes from the δ^{18}O profiles of Krantz (1990). Annotated versions of these profiles are available online as Supplementary Data File 2, and other raw data as Supplementary Data File 3.

RESULTS AND ANALYSIS

Oxygen Isotope Data

Problematic Profiles.—Most of the $\delta^{18}O$ profiles in Figures 5–8, together with those obtained from *C. eboreus* by Krantz (1990), are of a form readily interpretable in terms of the seasonal temperature cycle. However, a few profiles present problems. The profile from EPLI-GCP 1 (Fig. 5A) shows only slight variation in $\delta^{18}O$ compared to another specimen of comparable size from the same division (EPLI-GCP 2; Fig. 5C). The similar or greater $\delta^{18}O$ values from EPLI-GCP 1 compared to winter values from EPLI-GCP 2 suggest that the former profile is a (somewhat 'noisy') record of winter alone, but microgrowth-increment data (see below) indicates that over a year is represented. Accepting the latter evidence, we have assumed that the modest reduction in $\delta^{18}O$ at approximately 45 mm shell height marks the second of two summer intervals, and have determined seasonal temperatures, and half- and whole-year shell increments, accordingly. The profile from LPLI-GCP 3 (Fig. 6C) shows even less variation and values intermediate between the winter and summer values of shells from the same division. Microgrowth-increment data indicates that this shell lived only a few months, hence it is entirely plausible that only one of these seasons is represented. We have assumed it to be winter because the $\delta^{18}O$ values are closer to the mean of maxima rather than minima from other shells of the same division. The profile from LPLI-GCP 2 (Fig. 6B) is problematic because it shows an excursion to high values (the highest in the profile) at about 75 mm, interrupting a smooth trend to low values. Rather than representing winter, it may be that these high values reflect a downturn in temperature during spring; such fluctuations are certainly evident in other profiles (e.g., at about 65 mm in LPLI-GCP 6; Fig. 6F). However, for consistency with the approach applied to other profiles we have assumed that the values around 75 mm are representative of winter and have determined seasonal temperatures and half- and whole-year increments in accordance with this. A final problem is represented by abrupt excursions to lower values in early ontogeny, in some cases to the lowest values in the profiles (starred values in Figs. 6A, 6E, 7D). If these values are taken to represent summers the adjacent inflections have to be interpreted as winters. However, the values involved in the inflections are inconsistent with this, being much lower than clear winter values later in the profiles. It seems probable that the early ontogenetic $\delta^{18}O$ excursions (which in the cases highlighted are matched by excursions in $\delta^{13}C$) reflect incorporation into samples of material from below the thin outer layer (see previous section). The 'crystalline' material seen at shallow depths in the umbonal area could have been altered myostracal aragonite. If this had equilibrated with groundwaters of meteoric origin (typically low $\delta^{18}O$) and been incorporated into samples it would have imparted a lower $\delta^{18}O$ to them. In view of the likely diagenetic origin of early ontogenetic 'spikes', we have disregarded them in seasonal interpretation of $\delta^{18}O$ profiles and calculation of seasonal temperatures. It is worth mentioning here that there is little evidence from aberrant $\delta^{18}O$ values for alteration of outer-layer calcite.

Characteristics of Profiles.—We here itemise the general features of profiles and their life-history implications; the temperatures and specific overall growth rates implied are discussed later.

1. Only about half the profiles in Figures 5–8 show a full seasonal cycle and just two (LPLI-GCP 6, EPLE-MACP 1) show as much as 1.5 cycles. A similar proportion of the profiles obtained by Krantz (1990) show a full cycle, one (EPLE-MACP 4) showing about 1.5 cycles and another (EPLE-MACP 9) about 1.75 cycles. Since the latter profile starts at a shell height above 20 mm, it is conceivable that a complete ontogenetic profile would have shown two full cycles. It appears therefore that *C. eboreus* lived no longer than two years, in

some cases (e.g., LPLI-GCP 6; height 165 mm, age 1.5 years) reaching a very large size in a shorter time.

2. Amongst the profiles from the MACP in Figures 5, 7 and 8, all start at or somewhat before a summer minimum (i.e., post-larval growth commenced in the spring or summer), that from LPLI-MACP 5 starting earliest but clearly on a declining trend. While some from the GCP in Figures 5, 6 and 8 start a little before (but never at) a summer minimum, the profiles from EPLI-GCP 1 and 2, LPLI-GCP 6 and EPLE-GCP 2 (and probably also LPLI-GCP 2 and 3) start at or somewhat before a winter maximum (i.e., in the fall or winter), that from LPLI-GCP 6 starting earliest, at a value considerably less than the winter maximum. The profiles provided by Krantz (1990), all from the MACP, start at a shell height of 15 mm or more so it is impossible to be sure about the time of onset of growth. However, since all start at low $\delta^{18}O$ values, and some show a subsequent fall, it is likely that post-larval growth commenced in the spring or summer.

3. Only a few profiles terminate (i.e., the individual died) in summer (e.g., LPLI-GCP 2, LPLI-MACP 6) and many in winter. However, of the six largest individuals (height > 120 mm), five died during the spring rise in temperature (LPLI-GCP 1, 5, 6; LPLI-MACP 1; EPLE-GCP 1). Since these individuals were evidently not compromised by low temperatures, would have been relatively immune from predation through their size (see earlier discussion), and were still young, they possibly died after their first reproductive (spawning) event—i.e., *C. eboreus* may have been semelparous (Cole 1954). High winter mortality at smaller sizes might reflect a cold-induced lowering of swimming capacity and consequent reduced ability to escape predators by this means (see earlier discussion).

4. Of the profiles in Figures 5–8, only that for EPLE-MACP 1 is close to sinusoidal, all but one of the rest having a low gradient (falling and rising values) for the first half to whole cycle and then steepening markedly (LPLI-GCP 6 is unusual in showing a steep rise in values

in earliest ontogeny, succeeded by a gradual fall). Two (EPLE-MACP 4, 9) of the profiles provided by Krantz (1990) are close to sinusoidal but others that span a sufficient interval show the same ontogenetic increase in steepness, which indicates a decline in growth rate. It is noteworthy that the more sinusoidal profiles are all ones extending well into a second year and show relatively small half- and whole-year increments (Table 2). Longer life is a common corollary of slower growth amongst bivalves (Moss et al. 2016).

5. Where profiles are distinctly non-sinusoidal, the winter sectors are typically narrower (indicating slower growth) than the summer. Exceptions to this rule are specimens from the GCP showing a fall or winter start to growth (e.g., EPLI-GCP 2). The broad 'spring' sector in the profile from LPLI-MACP 5, a specimen showing an unusually early start to growth for its location, suggests that it is the time of growth onset rather than geographic position that is critical in determining the relative amounts of winter and summer growth over the ontogeny of an individual.

6. The sizes (heights) of the largest half- and whole-year increments (Table 2) are extremely variable: 16.0–121.7 mm for full half-years and 26.0–145.7 mm for full whole-years. The minimum estimates recorded are well below the upper limits of these ranges so it is unlikely that the actual increment sizes exceeded them. The largest values for half- and whole-year increment size (i.e., fastest growth rates) in *C. eboreus* are 1.6 times the maximum values recorded amongst all other scallop species: 75 mm for half-year increment size in modern wild *Ylistrum balloti* (Williams and Dredge 1981); 90 mm for whole-year increment size in modern cultured *Argopecten prpuratus* (DiSalvo et al. 1984).

Stable Carbon Isotope Data

Amongst the $\delta^{13}C$ profiles in Figures 5–8, nearly all from the larger shells (height ≥ 100 mm), exhibit ontogenetic trends to lower values (reaching –5.03‰ in EPLE-GCP 1), superimposed on which are more or less pronounced fluctuations, paralleling those in $\delta^{18}O$ profiles. However, in the large shell LPLI-GCP1 there is no overall reduction in $\delta^{13}C$ and downward fluctuations do not parallel $\delta^{18}O$. The last of the downward fluctuations corresponds to a $\delta^{18}O$ maximum, thus conforming to the expectations of an upwelling event (Jones and Allmon 1995). However, the $\delta^{18}O$ maximum is at the end of a long-term trend to higher values and so is much more reasonably interpreted as the culmination of winter cooling rather than incursion of cool deep-waters. Excursions to lower $\delta^{13}C$ earlier in ontogeny are not mirrored by excursions to higher $\delta^{18}O$, although the trend to increasing $\delta^{18}O$ is slightly steepened. This may reflect slower growth, as suggested by contemporaneous reductions in microgrowth-increment size.

In shells less than 100 mm in height, $\delta^{13}C$ generally lies between –1.00 and +1.00‰, in some cases fluctuating in accordance with $\delta^{18}O$ (e.g., EPLI-MACP 2), in certain others showing a slight ontogenetic increase (not in accordance with $\delta^{18}O$; e.g., LPLI-MACP 4), and in yet others essentially 'flat-lining' (e.g., LPLI-GCP 4). The range of values and patterns from the smaller shells is very much like that obtained by Krantz (1990) from LPLI-MACP and EPLE-MACP shells up to 100 mm. As in the larger shells, there is no evidence of upwelling from inverse variation in $\delta^{13}C$ relative to $\delta^{18}O$ (cf. Jones and Allmon 1995).

For the smaller shells represented in Figures 5–8 and the first 100 mm of ontogeny of the larger shells, mean $\delta^{13}C$ ranges from –1.90 ± 0.66 (± 1σ) to +0.89 ± 0.24‰ (EPLE-GCP 1 and LPLI-MACP 4, respectively). Grand means from these shells for each of the time-space divisions are as follows: EPLI-GCP: +0.08 ± 0.08‰; EPLI-MACP: –0.26 ± 0.22‰; LPLI-GCP: –0.11 ± 0.69‰; LPLI-MACP: +0.49 ± 0.32‰; EPLE-GCP: –1.36 ± 0.54‰: EPLE-MACP: –0.14 ± 0.09‰. The EPLI-GCP, EPLI-MACP and LPLI-GCP values are substantially lower than the individual averages from two modern specimens of the scallop *Placopecten magellanicus* from the Middle Atlantic Bight, and also lower than the individual averages from two of three modern specimens of the scallop *Argopecten gibbus* from the South Atlantic Bight (Krantz et al. 1988). This is consistent with the high primary production inferred for these divisions, since, whether the necessary nutrients were derived by upwelling or fluvial supply, they would have been associated with dissolved carbon of low δ^{13}C. The higher LPLI-MACP grand mean is correspondingly consistent with the ‘average’ production inferred for this division. The negative EPLE-MACP value is not consistent with the ‘average’ production inferred but is evidently a reflection of small sample size: nearly all the individual averages of the EPLE-MACP specimens analysed by Krantz (1990) are positive. Small sample size may likewise account for the negative EPLE-GCP grand mean, but the value is so low that it brings into question the ‘average’ production inferred.

In conclusion, the δ^{13}C data provides scant evidence of short-term upwelling events, but in the low individual averages contributing to low grand means they may evince more protracted supply of nutrient-rich waters capable of supporting high production. Ontogenetic fluctuations in δ^{13}C paralleling δ^{18}O probably reflect the interaction between seasonal cycles of phytoplankton production and water-column stratification in a mid- to outer-shelf setting (Arthur et al. 1983; Johnson et al. 2017; Vignols et al. 2018).

Microgrowth Increments

Microgrowth-increment profiles are only available for the specimens in Figures 5–8. Despite high frequency, relatively low amplitude variation, most profiles that are sufficiently long show a major (high amplitude) cycle of size change—from small to large to small—within the height interval of the first δ^{18}O cycle, with increments remaining small thereafter.

The microgrowth-increment cycle commonly occupies substantially less than the height interval of the first $\delta^{18}O$ cycle (which may be incomplete), such that the cycles are out of phase. At least for the LPLI interval, for which the most data is available, this pattern is evident in shells from both the MACP (e.g., LPLI-MACP 2 and 4) and GCP (e.g., LPLI-GCP 6). Maximum microgrowth-increment size typically corresponds to low or rising $\delta^{18}O$ in shells from the MACP and high or falling $\delta^{18}O$ in shells from the GCP. However, this is clearly not a reflection of geographic differences in the time of optimum growth conditions but rather of the onset of growth (see above), because most exceptions to the pattern show unusually early (LPLI-MACP 5) or late (LPLI-GCP 5, EPLE-GCP 1) starts to growth for their respective areas. Short-term increases and decreases in increment size are matched by increases and decreases in $\delta^{13}C$ in some shells (e.g. LPLI-GCP 1, LPLI-MACP 5, EPLE-GCP 1) but not by any notable changes (increases or decreases) in $\delta^{18}O$ over the same height interval. They therefore do not relate to temperature. The correlation with $\delta^{13}C$ over short intervals may manifest the same process as the mutual declines in microgrowth-increment size and $\delta^{13}C$ over the course of ontogeny. This could be greater incorporation of isotopically light respiratory carbon when growth rate is low, as represented by smaller microgrowth increments (Lorrain et al. 2004).

The data for microgrowth-increment size and number confirms that the half- and whole-year increments determined from $\delta^{18}O$ profiles do indeed represent time-intervals of these lengths—i.e., that shell $\delta^{18}O$ reflects seasonal temperature variation rather than extreme (and improbable) variation in water $\delta^{18}O$, over some unknown timescale. The major cycle of size change within the first $\delta^{18}O$ cycle is very comparable with the pattern in young, cultured examples of the living scallops *Aequipecten opercularis* and *Pecten maximus* (Broom and Mason 1978; Owen et al. 2002). In these, microgrowth-increment size increases from late winter to reach a summer maximum and then falls to a late fall minimum, succeeded by several months of little or no growth. Over the period in which the largest increments are formed, which is also the time of most rapid overall growth, the number laid down closely corresponds to the number of days elapsed (i.e., the microgrowth increments are 'daily'), as in some other scallop species (e.g., Joll 1988; Clark 2005; Velarde et al. 2015). Outside this period, fewer are laid down, such that there is an increasing discrepancy with the number of days elapsed as the time-interval expands. In *C. eboreus*, increment numbers in relation to δ^{18}O-defined time intervals (Table 2) exhibit similar features. The maximum number in a half-year interval (208; LPLI-GCP 5) slightly exceeds the number of days (183), but this could reflect inaccurate location of the summer δ^{18}O minimum: the summer sector of the profile concerned (Fig. 6E) is very broad and exhibits a little 'noise', making it possible that the position of the δ^{18}O minimum does not exactly correspond to the time of maximum temperature. The next highest count (164; LPLI-GCP 6) is from the specimen exhibiting the largest half-year increment (i.e., sustained rapid growth), with two other counts above 150. By contrast, while all whole-year counts are less than the number of days (365), the highest number is 247 (from a rapid grower; LPLI-GCP 5), representing a greater discrepancy with the number of days than the four highest half-year counts. As well as confirming the annual timescale of δ^{18}O cycles in *C. eboreus*, increment counts confirm the interpretations applied to problematic δ^{18}O profiles showing little or no cyclicality. The half- and whole-year increments recognised in EPLI-GCP 1 include 153 and 187 microgrowth increments, respectively. These counts are within the ranges set by other specimens showing more pronounced variation in δ^{18}O. Interpreting the entire δ^{18}O profile as a record from a single winter is inconsistent with the total increment count of 264, a number in excess of even the whole-year maximum in other specimens. The 'flat' δ^{18}O profile of LPLI-GCP 3 corresponds to 61 increments, a number consistent with its interpretation as a record from a single winter.

In some *C. eboreus* specimens, the absolute size of microgrowth increments is like that typical of scallop species (Fig. 1F, 1G) but in the majority it is substantially larger (Fig. 1E; Table 2). Discounting the highest mean values for half- and whole-year intervals (based on a small dataset from EPLI-MACP 1, in which microgrowth increments were difficult to measure), the next highest values—0.926 mm (LPLI-GCP 3) and 0.805 mm (LPLI-MACP 1), respectively—are still impressively high, being apparently approached only by *Oppenheimopecten vogdesi* amongst living scallops (Clark 2005). Since these values are from specimens that were evidently rapid growers (half-year increment > 68.7 mm and whole-year increment 116.5 mm, respectively) it might be concluded that rapid growth was brought about by deposition of larger microgrowth increments. However, one must consider the possibility that deposition of increments was more frequent (i.e., on a larger proportion of days). The relationship between half-/whole-year increment size and microgrowth-increment size and number is best examined initially in cases where the half-/whole-year increment size has been precisely defined (from δ^{18}O profiles with sufficient summer/winter inflections), but including microgrowth-increment data which does not fully span the relevant half-/whole-year interval. Inclusion of this data boosts sample size and is unlikely to bias mean microgrowth-increment size, although it will of course incorporate underestimates of number. Figure 9A-D shows bivariate plots of this data, revealing fairly good correlations between microgrowth-increment number and half- and whole-year increment size (Fig. 9A, 9C, respectively), but effectively no correlation between mean microgrowth-increment size and half- or whole-year increment size (Fig. 9B, 9D, respectively). Using all the data (i.e., including minimum estimates for half- and whole-year increment sizes) yields slightly better correlations between microgrowth-increment number and half- and whole-year increment size (Fig. 9E, 9G, respectively), possibly because of the inclusion of shells where the height ranges of microgrowth-increment and δ^{18}O profiles are relatively closely matched. However, there is still no correlation between mean microgrowth-increment size and half- or whole-year increment size (Fig. 9F, 9H, respectively). It therefore seems clear that larger half- and whole-year increments (i.e., faster growth rates) generally resulted from deposition of more rather than larger microgrowth increments. Perhaps the fundamental daily rhythm was modulated by the availability of sufficient energetic and material resources to cater for shell secretion as well as soft tissue (including gonad) growth and metabolic needs—i.e., the resources of environments occupied by relatively slow growers only allowed deposition of a new microgrowth increment several days after formation of the previous one. Certainly, deposition is not tied to a one-day periodicity in scallops (Thébault et al. 2006).

Growth Breaks

Significant (major and moderate) growth breaks occur over the full height interval of the major microgrowth increment cycle in some of the shells represented in Figures 5–8 (e.g., LPLI-MACP 2, EPLE-MACP 2). However, in most instances they are concentrated near or at the end, continuing to occur amongst any later (typically small) increments (e.g., LPLI-GCP 6). Amongst the shells represented in Figures 5–8, significant growth breaks occur close to the positions of δ^{18}O maxima and minima (including the highest maxima and lowest minima) in almost equal proportions, with no difference between GCP and MACP shells. Those occurring at locations away from δ^{18}O maxima and minima are not associated with notable changes of profile gradient. They and others may therefore signify only brief interruptions of growth. Amongst the 12 MACP shells studied by Krantz (1990), major growth breaks are associated with the highest δ^{18}O maximum in five cases (LPLI-MACP 8, EPLE-MACP 7–10) but with the lowest minimum in only one (EPLE-MACP 4).

Winter and Summer Benthic Temperatures

Preliminary considerations.—As well as diagenesis, noise and possible misidentification of winter and summer sectors in $\delta^{18}O$ profiles (see above), ontogenetic and seasonal changes in growth rate (including growth breaks) and profile truncation are matters which must be considered in interpreting seasonal temperatures from $\delta^{18}O$ data.

Ontogenetic decline in growth rate is typical of bivalves and confirmed in *C. eboreus* by the change in form of $\delta^{18}O$ profiles (generally steeper in late ontogeny). While closer isotopic sampling in late ontogeny no doubt did something to maintain temporal resolution, the higher $\delta^{18}O$ minima in the second year of growth (five of the six cases where two minima have been recognised; Table 3) suggest that it was not wholly effective: it seems likely that shell material formed at the time of highest temperature was not sampled. We have therefore taken the lowest $\delta^{18}O$ minimum from each shell (rather than the mean of two values, if available) as representative of summer conditions during the life of the individual and, for consistency of approach, taken the highest $\delta^{18}O$ maximum as representative of winter conditions, even though no age-related resolution effect is evident amongst winter data.

Seasonal change in growth rate (indicated by the relative widths of winter and summer sectors in $\delta^{18}O$ profiles) and growth breaks are evident in most shells. Growth was usually slower in winter and, like slowing of growth in late ontogeny, may have led to a failure to sample material formed under the most extreme temperatures of the season. Growth breaks associated with $\delta^{18}O$ maxima and minima may have been of brief duration (see above), such that the measured $\delta^{18}O$ values are not seriously misrepresentative. However, their higher relative occurrence in association with maxima amongst the MACP shells of Krantz (1990) could have led, in combination with winter slowing of growth, to more frequent underestimation of winter values from these $\delta^{18}O$ profiles.

$\delta^{18}O$ profiles are truncated at the highest value in EPLI-MACP 2, LPLI-MACP 2, 4 and 5, and EPLE-MACP 1 and 3, and at the lowest value in LPLE-MACP 7 and EPLE-MACP 1, 3 and 7. The former and latter sets of cases are likely to provide, respectively, underestimates of extreme winter values and overestimates of extreme summer values. It is noteworthy that all are from the MACP and that probable winter underestimates form the larger proportion. Similar numbers and proportions of cases exist where profiles are truncated near the highest and lowest values (i.e., where the adjacent inflection in the $\delta^{18}O$ profile may actually represent noise rather than a change in the sign of temperature change). These include a few cases from the GCP, with an equal proportion of possible winter underestimates (LPLI-GCP 4, EPLE-GCP 2) and possible summer overestimates (EPLI-GCP 1, LPLI-GCP 2).

Seasonal temperatures.—The following discussion uses temperatures calculated with the preferred water $\delta^{18}O$ value for the division concerned (Table 3). The full dataset (including temperatures calculated with the other three water $\delta^{18}O$ values applied in each case) is available online as Supplementary Data File 4.

Since they were part of the dataset used at the outset to define the high and low temperature ranges for winter and summer, it is no surprise that 11 of the 12 shells isotopically investigated by Krantz (1990) yield temperatures within the expected categories: HS/HW for LPLI-MACP 8; LS/LW for EPLE-MACP 3–12. That LPLI-MACP 7 does not (falling within the LS/HW category) is a consequence of the use of mean rather than individual data to define the boundary between high and low temperatures, and the fact that the high summer $\delta^{18}O$ value supplied by this particular specimen is from the end of a profile and almost certainly an overestimate, as already noted by Krantz (1990).

Of the other 20 shells considered herein, only eight yield temperatures within the expected category (EPLI-GCP 2; EPLI-MACP 1, 2; LPLI-GCP 2–4; EPLE-MACP 1, 2), the remainder giving temperatures in the low rather than high range for winter and/or summer, with the single exception of EPLE-GCP 1 (yielding a high rather than low summer temperature). Temperatures that are unexpectedly low for winter (EPLI-GCP 1; LPLI-GCP 1, 5, 6; LPLI-MACP 2, 5, 6; EPLE-GCP 2) cannot be the result of slower growth, growth breaks or truncation of δ^{18}O profiles, all of which would lead if anything to overestimates of winter temperature. However, these factors might in principle account for lower than expected summer temperatures, so such cases (LPL1-GCP 5, 6; LPLI-MACP 1-7) need to be considered further. In only one (LPLI-MACP 7) is the summer δ^{18}O value involved from an atypical (narrow) summer sector or the end/near-end of a profile, and in three of the others (LPLI-GCP 5; LPLI-MACP 4, 6) there is no significant growth break associated. Growth breaks are, however, located close to the positions of the lowest δ^{18}O values in LPLI-GCP 6, LPLI-MACP 1-3 and LPLI-MACP 5. It is doubtful whether temperatures well below the HS range (LPLI-GCP 6; LPLI-MACP 1; LPLI-MACP 2; LPLI-MACP 7:) reflect overestimation of δ^{18}O as a consequence of truncation or growth breaks. However, where summer temperatures are just below the HS/LS boundary (LPLI-MACP 3; LPLI-MACP 5) this is a distinct possibility. LPLI-MACP 3 may, therefore, have lived under HS/HW conditions and LPLI-MACP 5 under HS/LW conditions. LPLI-GCP 4, LPLI-MACP 1, 3 and 4, and EPLE-GCP 1 yield winter temperatures within the HW range, as expected, but the values concerned are within 1 °C of the HW/LW threshold and correspond to δ^{18}O values from positions near to growth breaks and/or the ends of profiles. It is therefore possible that temperatures fell to values within the LW range. The general picture is of temperatures according with expectation or lower, there being just one example of a higher (summer) temperature than expected, two examples where a more complete δ^{18}O record might have yielded a higher (summer) temperature than expected, and a further five examples where a more complete δ^{18}O record might have yielded a lower (winter) temperature than expected.

While the seasonal temperatures calculated from shells are changed if the value for water $\delta^{18}O$ is altered, the discrepancies with expectation identified above remain if the expected temperatures are recalculated with the altered value for water $\delta^{18}O$ (not applicable to EPLI-GCP, where the expected temperatures are based on assemblage composition). It is nevertheless worth examining the influence of water $\delta^{18}O$ on the absolute temperatures obtained from shells. Winter and summer temperatures calculated using an arbitrary common value of water $\delta^{18}O$ (+0.7‰) are presented in Table 3 for comparison with those calculated using the preferred values. The effect of a common water $\delta^{18}O$ on divisional mean temperatures is to make the EPLE-GCP winter temperature relatively high and the other winter temperatures relatively low, and the LPLI-GCP, EPLE-GCP and EPLE-MACP summer temperatures relatively high and the EPLI-GCP, EPLI-MACP and LPLI-MACP summer temperatures relatively low. While ostracod and mollusk assemblages provide independent evidence of warm conditions for the EPLE-MACP division, the indicated temperatures are little or no higher than in the LPLI-MACP division (Hazel 1971, 1988; Ward et al. 1991). More significantly, ostracod and mollusk assemblages, together with foram assemblages (Dowsett and Wiggs 1992), provide compelling evidence that temperatures were substantially higher in the LPLI-MACP division than in the EPLI-MACP division, in notable contrast to $\delta^{18}O$ data from *C. eboreus* employed with a common value of water $\delta^{18}O$. It is evident from this analysis that water $\delta^{18}O$ has a considerable impact on estimated temperature, but also clear that use of a common value is inappropriate. We made informed choices for each division (see above) but recognise that it would be worth applying additional methods to constrain water $\delta^{18}O$. 'Clumped isotope' (Δ_{47}) analysis (e.g., Winkelstern et al. 2017) and the $\delta^{18}O$ of homeotherm phosphate (e.g., Walliser et al. 2015; Ciner et al. 2016) are promising tools.

Growth Rate-Environment Relationships

Based on their largest half-year (hy) and whole-year (wy) increment sizes we have assigned shells to growth-rate classes as follows: Slow (hy < 30 mm, wy < 60 mm); Medium (hy > 30 mm, wy > 60 mm); Fast (hy > 60 mm, wy > 90 mm); Very Fast (hy > 90 mm, wy > 120 mm). In cases of conflict between half- and whole-year data we have assigned shells to the faster growth-rate class indicated. The growth-rate distribution amongst the 32 shells is 9 Slow, 14 Medium, 5 Fast, 4 Very Fast. Shells in the Slow class are restricted to the MACP and those in the Very Fast class to the GCP. Figure 10 locates the shells, segregated by growth rate, within the temperature/primary production matrix previously generated (Fig. 4), but in positions informed by the isotopic data obtained from them. As indicated above, δ^{18}O data places many shells in a different temperature category to that expected, and more complete records might have had the same effect for a number of other shells. The latter possibility is indicated by a second entry in smaller typeface at the appropriate position. The same approach is used with respect to production category in the cases of EPLE-GCP 1 and 2, for which δ^{13}C data provides some evidence of high rather than 'average' production. Otherwise, we have assigned shells to the production category indicated by the associated fauna (see above).

Reasoning from the growth-rate predictions set out earlier, and defining 'rapid' growth as a rate within the Very Fast class (faster growth than in any other scallop species), the existence of examples (LPLI-GCP 5, 6) from the LS/LW temperature category rules out temperature control of growth. The existence of an example (EPLE-GCP 1) from the 'average' production category appears to rule out production control as well. However, the growth rate of this specimen is only just in the Very Fast class and, as we have noted, δ^{13}C evidence from the division concerned (and this specimen in particular) provides some grounds for thinking that production may have been high rather than 'average'. Defining 'rapid' more broadly to include the Fast growth-rate class gives a more ambiguous picture: two definite examples and one possible are added from the LS/LW temperature category but also three definite examples from the 'average' production category. This is, however, consistent with the environmental associations of modern scallops in the Fast growth-rate class: populations of *Y. balloti* and *A. purpuratus* exhibiting this rate of growth occur in areas of 'average' phytoplankton production (FAO 1981, map 1.1) in north-eastern Australia and northern Chile, respectively (Williams and Dredge 1981; DiSalvo et al. 1984).

That there are a number of examples of Medium growth rate from the high production category does not refute the notion of production-controlled growth: some variation in growth rate is to be expected due to short-term fluctuations in production and to individual differences in the ability to respond to high food supply. Moreover, the proportion of examples of Medium growth rate relative to cases of Fast and Very Fast growth rate is no lower in the HS/HW than in the LS/LW temperature category, contrary to what one would expect for temperature-controlled growth. Support for production-controlled growth comes from the complete absence of examples of Slow growth from the high production category, in contrast to many from the 'average' production category. Amongst the latter, however, all but one are from the LS/LW temperature category. The δ^{18}O profile of the sole exception (LPLI-MACP 7) is short, apparently including a winter maximum (giving a temperature in the high winter range) but not showing a summer inflection and therefore providing only a minimum estimate (> 20 mm) for half-year increment. The growth rate of this specimen might therefore actually have been in the Medium class. Not only are there many in the Slow growth-rate class within the LS/LW temperature category, the winter minimum temperatures supplied are notably low: four of eight below 7 °C (Table 3) compared with none as low as this amongst the six Medium–Very Fast growers from the same temperature category under high or possibly high production. The winter temperature supplied by the Very Fast grower LPLI-GCP 1, also from a high production setting but in the HS/LW temperature category, is also relatively high (11.3 °C). In this case there is no growth break associated with the winter temperature minimum, but one is present in the other specimens from high production/low winter temperature settings. These individuals may therefore have experienced (but not recorded) winter temperatures approaching those indicated by some of the Slow growers in the LS/LW temperature category and 'average' production category. By their very existence, however, winter growth breaks (and the slowing of growth in this season) show some control of growth by temperature as well as production. Such breaks are more common than summer growth breaks amongst shells from the EPLE-MACP division, from which all definite examples of Slow growth derive. It is therefore reasonable to conclude that these examples reflect the influence of low winter temperature, in addition to 'average' production.

CONCLUSIONS AND FURTHER WORK

We have shown that *C. eboreus* lived no longer than two years but in some cases grew exceedingly rapidly (by depositing more rather than larger microgrowth increments) to reach an unusually large size. Growth typically slowed in winter, when mortality was relatively high, and in late ontogeny. Individuals surviving long enough to spawn may then have suffered a 'programmed' death. Post-larval growth started in the spring or summer in the MACP, but sometimes in the fall or winter in the GCP; growth interruptions occurred in summer and winter in both areas, but more commonly in winter in the former. As well as these geographic differences in life history, overall growth rate varied with specific aspects of the environment (primary production and temperature).

On the basis of growth rate-environment relationships we may interpret the extinction of *C. eboreus* as a result of the combined impact of declines in primary production and temperature, specifically winter temperature. The lower growth rate associated with these changes would have increased mortality through predation by preventing rapid achievement of the refuge offered by large size. This might have led to a progressive reduction in overall population size. The lack of impact of low temperature on growth under conditions of high production implies that extinction would not have occurred had these conditions been maintained. On the other hand, the evident impact of low temperature on growth under 'average' production suggests that if temperature had been maintained, reduced production might have been insufficient to cause extinction. The survival (in abundance) of *C. eboreus* in the MACP long after the fall in production within the Pliocene seems to confirm that temperature decline was contributory to extinction. However, it is puzzling that the species continued deep into the Pleistocene, by which time there had been numerous, increasingly severe, episodes of refrigeration in the North Atlantic region (McClymont et al. 2013). There is some evidence for a Pleistocene reduction in predation intensity on bivalves in the GCP (Mondal et al. 2014) but not in the MACP (Sime and Kelley 2016), so it cannot be argued that growth-related decline in the ability of *C. eboreus* to survive predatory attacks was offset by less frequent encounters with predators. Perhaps the continuation of the species reflects localised persistence of high production and/or the time required for disruption of once-ubiquitous high production over the geographic range of *C. eboreus* to bring about the demise of all populations. Certainly, the effects of habitat fragmentation and reduction are not immediate, and (counter-intuitively) extinction of competitively inferior species may be especially delayed (Nee and May 1992; Tilman et al. 1994). Short larval life also confers resistance to extinction in scallops (Smith and Jackson 2009). The competitive status of *C. eboreus* would be difficult to determine but duration of the larval stage is straightforward

(Smith et al. 2003). As well as the latter, it would be well worth investigating the growth rate and environment of the very latest recorded specimens, from the Flanner Beach and Canepatch formations. Individuals up to 156 mm in height are known (Ward 2008, pl. 16, figs. 1, 2), a size reached earlier only under high production, hence these examples might evince the localised persistence of such conditions, as hypothesised above. Demonstration of rapid growth by the techniques employed herein would support this interpretation, and it might be confirmed (in the absence of assemblage evidence) by various other geochemical approaches (e.g., Krantz et al. 1988; Haveles and Ivany 2010; Thébault and Chauvaud 2013; Georgiev et al. 2015). Conceivably, the indications from the latter might be that production was high, from δ^{18}O and microgrowth-increment profiles that growth was slow, and from absolute δ^{18}O values that temperature was low. This would lend support to the involvement of temperature decline in extinction whilst also maintaining a role for production decline. Temperature estimates from shell δ^{18}O would, however, be subject to the same uncertainty as those obtained from older material herein. For this reason, incorporation of the additional (but still isotope-based) approaches advanced earlier would be beneficial. Indeed, the conclusions reached from the present study are to some extent dependent on the accuracy of the temperatures determined, and these therefore urgently need validation by the additional approaches advocated. If it were shown that EPLE-MACP specimens in the Slow growth-rate class lived under warm winter conditions (in agreement with mollusk- and ostracod-assemblage evidence but contrary to the δ^{18}O-derived temperatures supplied herein), it would remove the case for some involvement of temperature decline in the extinction of *C. eboreus*.

Ultimately, companion sclerochronological studies of other taxa will be required to formulate a general theory of Plio-Pleistocene bivalve extinction on the US eastern seaboard. As indicated at the outset, hundreds of species became extinct, and *C. eboreus* may constitute an exception in having been adversely affected by reduced primary production. However, the same cause has been invoked for the selective demise of a large, fast-growing *Crassostrea* species in the Pliocene of the Caribbean (Kirby and Jackson 2004) and might also apply to the extinction of *Chesapecten*, a further large, fast-growing scallop taxon (Goewert and Surge 2008), in the Pliocene of the US eastern seaboard. Other large taxa survived from the Pliocene to present. Possibly these were unaffected by reduced production as a result of a life-history strategy involving slow growth and long life. Such a strategy might have been advantageous (enabling greater investment in reproduction) if the predators of these taxa were not deterred by large size. In *Mercenaria*, several species of which survived from the Pliocene to present, large size does offer a refuge from predation (Dietl 2003), so slow growth would have been disadvantageous. Whether large size has benefits in other taxa is in most cases only surmised. Certainly, sclerochronological studies will need to be accompanied by aut- and synecological investigations (cf. Dietl et al. 2004; O'Dea and Jackson 2009; Smith and Jackson 2009; Leonard-Pingel et al. 2012; Leonard-Pingel and Jackson 2016; Sime and Kelley 2016) for a full understanding of Plio-Pleistocene bivalve extinction on the US eastern seaboard.

ACKNOWLEDGMENTS

We are very grateful to Lauck ('Buck') Ward and Alex Hastings (Virginia Museum of Natural History), and to Roger Portell (Florida Museum of Natural History), for the loan of specimens in their care for investigation. Ward and Portell also advised on provenance and kindly arranged and guided field visits by ALAJ, as did Justin McNabb (University of North Carolina at Chapel Hill). We thank Michael Maus for assistance with isotopic analysis at Mainz; Richard Duff and Matt Hunt for other technical support; Harry Dowsett, Joel Hudley, Jon Todd and Tom Waller for helpful discussions during the course of the research; and the reviewers and editors for detailed, constructive comments which improved the clarity and content of the paper. The work was partially supported by a PhD studentship award to AMV under the University Funding Initiative of the British Geological Survey (BUFI S157), a grant of analytical services to ALAJ through the NERC Isotope Geoscience Facilities Steering Committee (IP-1351-1112), and a travel award to ALAJ from the Research-Inspired Curriculum Fund of the University of Derby.

REFERENCES

ABELE, D., BREY, T., and PHILLIP, E., 2017, Ecophysiology of extant marine Bivalvia, *in* Selden, P.A. (ed.), Treatise Online 92 (Part N, Revised, Volume 1, Chapter 7): Paleontological Institute, The University of Kansas, p. 1–50.

ALLMON, W.D., 1993, Age, environment and mode of deposition of the densely fossiliferous Pinecrest Sand (Pliocene of Florida)—implications for the role of biological productivity in shell bed formation: PALAIOS, v. 8, p. 183–201, doi: 10.2307/3515171.

ALLMON, W.D., 2001, Nutrients, temperature, disturbance, and evolution: a model for the late Cenozoic marine record of the western Atlantic: Palaeogeography, Palaeoclimatology, Palaeoecology, v. 166, p. 9–26, doi: 10.1016/S0031-0182(00)00199-1.

ALLMON, W.D., 2011, Natural history of turritelline gastropods (Cerithiodea, Turritellidae): A status report: Malacologia, v. 54, p. 159–202, doi: 10.4002/040.054.0107.

ALLMON, W.D. and DOCKERY, D.T., 1992, A turritelline gastropod-dominated bed in the Byram Formation (Oligocene) of Mississippi: Mississippi Geology, v. 13, p. 29–35.

ALLMON, W.D., ROSENBERG, G., PORTELL, R.W., and SCHINDLER, K.S., 1993, Diversity of Atlantic coastal plain mollusks since the Pliocene: Science, v. 260, p. 1626–1629, doi: 10.1126/science.260.5114.1626.

ALLMON, W.D., SPIZUCO, M.P., and JONES, D.S., 1995. Taphonomy and paleoenvironment of two turritellid-gastropod-rich beds, Pliocene of Florida: Lethaia, v. 28, p. 75–83, doi: 10.1111/j.1502-3931.1995.tb01594.x.

ALLMON, W.D., EMSLIE, S.D., JONES, D.S., and MORGAN, G.S, 1996, Late Neogene oceanographic change along Florida's west coast: Evidence and mechanisms: Journal of Geology, v. 104, p. 143–162.

ANDERSON, B.M., HENDY, A., JOHNSON, E.H., and ALLMON, W.D., 2017, Paleoecology and paleoenvironmental implications of turritelline gastropod-dominated assemblages from the Gatun Formation (Upper Miocene) of Panama: Palaeogeography, Palaeoclimatology, Palaeoecology, v. 470, p. 132–146, doi: 10.1016/j.palaeo.2017.01.026.

ARSENAULT, D.J. and HIMMELMAN, J.H. 1996. Size-related changes in vulnerability to predators and spatial refuge use by juvenile Iceland scallops *Chlamys islandica*: Marine Ecology Progress Series, v. 140, p. 115-122.

ARTHUR, M.A., WILLIAMS, D.F., and JONES, D.S., 1983, Seasonal temperature-salinity changes and thermocline development in the mid-Atlantic Bight as recorded by the isotopic composition of bivalves: Geology, v. 11, p. 655–659, doi: 10.1130/0091-7613(1983)11<655:STCATD>2.0.CO;2.

BRACHERT, T.C., REUTER, M., KRÜGER S., LOHMANN, H., PETUCH, E.J., and KLAUS, J.S., 2014, 4.2 million years record of interglacial paleoclimate from sclerochronological data of Florida carbonate platform (Early Pliocene to recent): Global and Planetary Change, v. 120, p. 54–64, doi: 10.1016/j.gloplacha.2014.06.001.

BRAND, A.R., 1991, Scallop ecology: distributions and behaviour, *in* Shumway, S.E. (ed.), Scallops: Biology, Ecology and Aquaculture. Developments in Aquaculture and Fisheries Science 21: Elsevier, Amsterdam, The Netherlands and New York, p. 517–584.

BRICELJ, V.M. and SHUMWAY, S., 1991, Physiology: energy acquisition and utilization, *in* Shumway, S.E. (ed.), Scallops: Biology, Ecology and Aquaculture. Developments in Aquaculture and Fisheries Science 21: Elsevier, Amsterdam, The Netherlands and New York, p. 305–346.

BROOM, M.J. and MASON, J., 1978, Growth and spawning in the pectinid *Chlamys opercularis* in relation to temperature and phytoplankton concentration: Marine Biology, v. 47, p. 277–285.

CAMPBELL, L.D., 1993, Pliocene molluscs from the Yorktown and Chowan River formations in Virginia: Commonwealth of Virginia (Virginia Division of Mineral Resources, n. 127), Charlottesville, 259 p.

CINER, B., WANG, Y., and PARKER, W., 2016, Oxygen isotopic variations in modern cetacean teeth and bones: implications for ecological, paleoecological, and paleoclimatic studies: Science Bulletin, v. 61, p. 92–104, doi: 10.1007/s11434-015-0921-x.

CLARK II, G.R., 2005, Daily growth lines in some living Pectens (Mollusca: Bivalvia), and some applications in a fossil relative: time and tide will tell: Palaeogeography, Palaoclimatology, Palaeoecology, v. 228, p. 26–42, doi: 10.1016/j.palaeo.2005.03.044.

COLE, L.C., 1954, The population consequences of life history phenomena: The Quarterly Review of Biology, v. 29, p. 103-137, doi: 10.1086/400074.

CRONIN, T.M. and DOWSETT, H.J., 1996, Biotic and oceanographic response to the Pliocene closing of the Central American Isthmus, *in* Jackson, J.B.C., Budd, A.F., and Coates, A.G., eds., Evolution and Environment in Tropical America: University of Chicago Press, Chicago, Illinois, p. 76–104.

DADSWELL, M.J. and WEIHS, D., 1990, Size-related hydrodynamic characteristics of the giant scallop *Placopecten magellanicus* (Bivalvia; Pectinidae): Canadian Journal of Zoology, v. 68, p. 778–785, doi: 10.1139/z90-112.

DIETL, G.P., 2003, Coevolution of a marine gastropod predator and its dangerous bivalve prey: Biological Journal of the Linnean Society, v. 80, p. 409–436, doi: 10.1046/j.1095-8312.2003.00255.x.

DIETL G.P., HERBERT G.S., and VERMEIJ, G.J., 2004, Reduced competition and altered feeding behavior among marine snails after a mass extinction: Science, v. 306, p. 2229-2231, doi: 10.1126/science.1106182.

DISALVO, L.H., ALARCÓN, E., MARTINEZ, E., and URIBE, E., 1984, Progress in mass culture of *Chlamys (Argopecten) purpurata* Lamarck (1819) with notes on its natural history: Revista Chilena de Historia Natural, v. 57, p. 35–45.

DOWSETT, H.J. and WIGGS, L.B., 1992, Planktonic foraminiferal assemblage of the Yorktown Formation, Virginia: Micropaleontology, v. 38, p. 75–86, doi: 10.2307/1485844.

DOWSETT, H.J., CHANDLER, M.A., and ROBINSON, M.M., 2009, Surface temperatures of the Mid-Pliocene North Atlantic Ocean: implications for future climate: Philosophical Transactions of the Royal Society, Series A, v. 367, p. 69–84, doi: 10.1098/rsta.2008.0213.

EMSLIE, S.D. and MORGAN, G.S., 1994, A catastrophic death assemblage and paleoclimatic implications of Pliocene seabirds of Florida: Science, v. 264, p. 684–685, doi: 10.1126/science.264.5159.684.

EMSLIE, S.D., ALLMON, W.D., RICH, F.J., WRENN, J.H., and DEFRANCE, S.D., 1996, Integrated taphonomy of an avian death assemblage in marine sediments from the late Pliocene of Florida: Palaeogeography, Palaeoclimatology, Palaeoecology, v. 124, p. 107–136, doi: 10.1016/0031-0182(96)00005-3.

EPSTEIN, S., BUCHSBAUM, R., LOWENSTAM, H.A., and UREY, H.C., 1953, Revised carbonate-water isotopic temperature scale: Bulletin of the Geological Society of America, v. 64, p. 1315–1326.

FAO (Food and Agriculture Organization of the United Nations, Fisheries Department), 1981, Atlas of the Living Resources of the Seas, 4th ed.: FAO, Rome, 23 p.

FIERSTINE, H.L., 2001, Analysis and new records of billfish (Teleostei: Perciformes: Istiophoridae) from the Yorktown Formation, early Pliocene of eastern North Carolina at Lee Creek Mine, *in* Ray, C.E. and Bohaska, D.J., eds., Geology and Paleontology of the Lee Creek Mine, North Carolina, III: Smithsonian Contributions to Paleobiology, n. 90, p. 21–70.

GEORGIEV, S.S., HORNER, T.J., STEIN, H.J., HANNAH, J.L., BINGEN, B., and REHKÄMPER, M., 2015, Cadmium-isotopic evidence for increasing primary productivity during the Late Permian anoxic event: Earth and Planetary Science Letters, v. 410, p. 84–96, doi: 10.1016/j.epsl.2014.11.010.

GIBBARD, P.L., HEAD, M.J., and WALKER, M.J.C., 2010, Subcommission on Quaternary stratigraphy. Formal ratification of the Quaternary System/Period and the Pleistocene Series/Epoch with a base at 2.58 Ma: Journal of Quaternary Science, v. 25, p. 96–102, doi: 10.1002/jqs.1338.

GIBSON, T.G., 1987, Miocene and Pliocene Pectinidae (Bivalvia) from the Lee Creek Mine and adjacent areas, *in* Ray, C.E. (ed.), Geology and Paleontology of the Lee Creek Mine, North Carolina, II: Smithsonian Contributions to Paleobiology, n. 61, p. 31–112.

GOEWERT, A.E. and SURGE, D., 2008, Seasonality and growth patterns using isotope sclerochronology in shells of the Pliocene scallop *Chesapecten madisonius*: GeoMarine Letters, v. 28, p. 327–338, doi: 10.1007/s00367-008-0113-7.

GONFIANTINI, R., STICHLER, W., and ROZANSKI, K., 1995, Standards and intercomparison materials distributed by the International Atomic Energy Agency for stable isotope measurements, *in* International Atomic Energy Agency, Reference and Intercomparison

Materials for Stable Isotopes of Light Elements: IAEA-TECDOC-825, Vienna, Austria, p. 13–29.

GOULD, S.J., 1971, Muscular mechanics and the ontogeny of swimming in scallops: Palaeontology, v. 14, p. 61–94.

HARPER, E.M., 2002, Plio-Pleistocene octopod drilling behavior in scallops from Florida: PALAIOS, v. 17, p. 292-296, doi: 10.1669/0883-1351(2002)017<0292:PPODBI>2.0.CO;2.

HARPER, E.M. and SKELTON, P.W., 1993, The Mesozoic Marine Revolution and epifaunal bivalves: Scripta Geologica, Special Issue 2, p. 127–153.

HARPER, E.M., PECK, L.S., and HENDRY, K.R., 2009, Patterns of shell repair in articulate brachiopods indicate size constitutes a refuge from predation: Marine Biology, v. 156, p. 1993–2000, doi: 10.1007/s00227-009-1230-1.

HAVELES, A.W. and IVANY, L.C., 2010, Rapid growth explains large size of mollusks in the Eocene Gosport Sand, United States Gulf Coast: PALAIOS, v. 25, p. 550–564, doi: 10.2110/palo.2009.p09-148r.

HAYAMI, I. and HOSODA, I., 1988, *Fortipecten takahashii*, a reclining pectinid from the Pliocene of north Japan: Palaeontology, v. 31, p. 419–444.

HAZEL, J.E., 1971, Paleoclimatology of the Yorktown Formation (upper Miocene and Lower Pliocene) of Virginia and North Carolina: Bulletin du Centre de Recherches de Pau, SNPA (Société Nationale de Pétroles d'Aquitaine), v. 5 (suppl.), p. 361–375.

HAZEL, J.E., 1988, Determining late Neogene and Quaternary palaeoclimates and palaeotemperature regimes using ostracods, *in* De Deckker, P., Colin, J.P., and Peypouquet, J.P. (eds.), Ostracoda in the Earth Sciences: Elsevier, Amsterdam, The Netherlands, p. 89–101.

JACKSON, J.B.C. and JOHNSON, K.G., 2000. Life in the last few million years: Paleobiology, v. 26 (Supplement), p. 221–235, doi: 10.1666/0094-8373(2000)26[221:LITLFM]2.0.CO;2.

JACKSON, J.B.C., JUNG, P., COATES, A.G., and COLLINS, L.S., 1993, Diversity and extinction of tropical American mollusks and emergence of the Isthmus of Panama: Science, v. 260, p. 1624–1626, doi: 10.1126/science.260.5114.1624.

JENKINS, S.R., LART, W., VAUSE, B.J., and BRAND, A.R., 2003, Seasonal swimming behaviour in the queen scallop (*Aequipecten opercularis*) and its effect on dredge fisheries: Journal of Experimental Marine Biology and Ecology, v. 289, p. 163–179.

JOHNSON, A.L.A., LIQUORISH, M.N., and SHA, J., 2007. Variation in growth-rate and form of a Bathonian (Middle Jurassic) oyster in England, and its environmental implications: Palaeontology, v. 50, p. 1155-1173, doi: 10.1111/j.1475–4983.2007.00698.x.

JOHNSON, A.L.A., HICKSON, J.A., BIRD, A., SCHÖNE, B.R., BALSON, P.S., HEATON, T.H.E., and WILLIAMS, M., 2009, Comparative sclerochronology of modern and mid-Pliocene (c. 3.5 Ma) *Aequipecten opercularis* (Mollusca, Bivalvia): an insight into past and future climate change in the north-east Atlantic region: Palaeogeography, Palaeoclimatology, Palaeoecology, v. 284, p. 164–179, doi: 10.1016/j.palaeo.2009.09.022.

JOHNSON, A.L.A., VALENTINE, A., LENG, M.J., SLOANE, H.J., SCHÖNE, B.R., and BALSON, P.S., 2017, Isotopic temperatures from the early and mid-Pliocene of the US Middle Atlantic Coastal Plain, and their implications for the cause of regional marine climate change: PALAIOS, v. 32, p. 250–269, doi: 10.2110/palo.2016.080.

JOLL, L.M., 1988, Daily growth rings in juvenile saucer scallops, *Amusium balloti* (Bernardi): Journal of Shellfish Research, v. 7, p. 73–76.

JONES, D.S. AND ALLMON, W.D., 1995, Records of upwelling, seasonality and growth in stable-isotope profiles of Pliocene mollusk shells from Florida: Lethaia, v. 28, p. 61–74, doi: 10.1111/j.1502-3931.1995.tb01593.x.

KAZÁR, E. and BOHASKA, D.J., 2008, Toothed whale (Mammalia: Cetacea: Odontoceti) limb bones of the Lee Creek Mine, North Carolina, *in* Ray, C.E., Bohaska, D.J., Koretsky, I.A., Ward, L.W., and Barnes, L.G. (eds.), Geology and Paleontology of the Lee Creek Mine, North Carolina, IV: Virginia Museum of Natural History Special Publication, n. 14, p. 271–324.

KIRBY, M.X. and JACKSON, J.B.C., 2004, Extinction of a fast-growing oyster and changing ocean circulation in Pliocene tropical America: Geology, v. 32, p. 1025–1028, doi: 10.1130/G21039.1.

KOHNO, N. and RAY, C.E., 2008, Pliocene walruses from the Yorktown Formation of Virginia and North Carolina, and a systematic revision of the North Atlantic Pliocene walruses, *in* Ray, C.E., Bohaska, D.J., Koretsky, I.A., Ward, L.W., and Barnes, L.G. (eds.), Geology and Paleontology of the Lee Creek Mine, North Carolina, IV: Virginia Museum of Natural History Special Publication, n. 14, p. 39–80.

KORETSKY, I.A. and RAY, C.E., 2008, Phocidae of the Pliocene of eastern USA, *in* Ray, C.E., Bohaska, D.J., Koretsky, I.A., Ward, L.W., and Barnes, L.G. (eds.), Geology and Paleontology of the Lee Creek Mine, North Carolina, IV: Virginia Museum of Natural History Special Publication, n. 14, p. 81–139.

KRANTZ, D.E., 1990, Mollusk-isotope records of Plio-Pleistocene marine paleoclimate, U.S. Middle Atlantic Coastal Plain: PALAIOS, v. 5, p. 317–335, doi: 10.2307/3514888.

KRANTZ, D.E., KRONICK, A.T., and WILLIAMS, D.F., 1988, A model for interpreting continental-shelf hydrographic processes from the stable isotope and cadmium:calcium profiles of scallop shells: Palaeogeography, Palaeoclimatology, Palaeoecology, v. 64, 123–140, doi: 10.1016/0031-0182(88)90002-8.

LEIGH E.G., O'DEA A. and VERMEIJ G.J., 2014, Historical biogeography of the Isthmus of Panama: Biological Reviews., v. 89, p.148-172, doi: 10.1111/brv.12048.

LEONARD-PINGEL, J.S. and JACKSON, J.B.C. 2016, Drilling predation increased in response to changing environments in the Caribbean Neogene: Paleobiology, v. 42, p. 394-409, doi: 10.1017/pab.2016.2.

LEONARD-PINGEL, J.S., JACKSON, J.B.C., and O'DEA, A., 2012, Changes in bivalve functional and assemblage ecology in response to environmental change in the Caribbean Neogene: Paleobiology, v. 38, p. 509-524, doi: 10.1666/10050.1.

LORRAIN, A., PAULET, Y.-M., CHAUVAUD, L., DUNBAR, R., MUCCIARONe, D., and FONTUGNE, M., 2004. δ^{13}C variation in scallop shells: Increasing metabolic carbon contribution with body size?: Geochimica et Cosmochimica Acta, v. 68, p. 3509–3519, doi: 10.1016/j.gca.2004.01.025.

MCCLYMONT, E.L., SOSDIAN, S.M., ROSELL-MELÉ, A., and ROSENTHAL, Y., 2013, Pleistocene sea-surface temperature evolution: Early cooling, delayed glacial intensification, and implications for the mid-Pleistocene climate transition: Earth Science Reviews, v. 123, p. 173–193, doi: 10.1016/j.earscirev.2013.04.006.

MILLER III, W.M., 1985, The Flanner Beach Formation (middle Pleistocene) in eastern North Carolina: Tulane Studies in Geology and Paleontology, v. 18, p. 93–122.

MONDAL, S., HARRIES, P.J., PAUL, S. and HERBERT, G.S., 2014, Paleoecological significance of coupling metrics of successful and unsuccessful shell-breaking predation: Examples using Neogene bivalve prey: Palaeogeography, Palaeoclimatology, Palaeoecology, v. 399, p. 89-97, doi: 10.1016/j.palaeo.2014.02.010.

MOSS, D.K., IVANY, L.C., JUDD, E.J., CUMMINGS, P.C., BEARDEN, C.E., KIM, J., ARTRUC, E.G., and DRISCOLL, J.R., 2016, Lifespan, growth rate, and body size across latitude in marine Bivalvia, with implications for Phanerozoic evolution: Proceedings of the Royal Society, Series B, v. 283, 20161364, 767 KB, doi:10.1098/rspb.2016.1364. Checked November 2018.

MOSS, D.K., IVANY, L.C., SILVER, R.B., SCHUE, J., and ARTRUC, E.G., 2017, High latitude settings promote extreme longevity in fossil marine bivalves: Paleobiology, v, 43, p. 365–382, doi: 10.1017/pab.2017.5.

NAKASHIMA, R., SUZUKI, A., and WATANABE, T., 2004, Life history of the Pliocene scallop *Fortipecten*, based on oxygen and carbon isotope profiles: Palaeogeography, Palaeoclimatology, Palaeoecology, v. 211, p. 299–307, doi: 10.1016/j.palaeo.2004.05.011.

NEE, S. and MAY, R.M., 1992, Dynamics of metapopulations: habitat destruction and competitive coexistence: Journal of Animal Ecology, v. 61, p. 37-40, doi: 10.2307/5506.

O'DEA, A., JACKSON, J B.C., FORTUNATO, H., SMITH, J.T., D'CROZ, L., JOHNSON, K.G., and TODD, J.A., 2007, Environmental change preceded Caribbean extinction by 2 million years: Proceedings of the National Academy of Sciences of the United States of America, v. 104, p. 5501–5506, doi: 10.1073/pnas.0610947104.

O’DEA A. and JACKSON J., 2009, Environmental change drove macroevolution in cupuladriid bryozoans: Proceedings of the Royal Society, Series B, v. 276, p. 3629-3634, doi: 10.1098/rspb.2009.0844.

OLSON, S.L. and HEARTY, P.J., 2003, Probable extirpation of a breeding colony of short-tailed albatross (*Phoebastria albatrus*) on Bermuda by Pleistocene sea-level rise: Proceedings of the National Academy of Sciences of the United States of America, v. 100, p. 12825–12829, doi: 10.1073/pnas.1934576100.

OLSON, S.L. and RASMUSSEN, P.C., 2001, Miocene and Pliocene birds from the Lee Creek Mine, North Carolina, *in* Ray, C.E. and Bohaska, D.J. (eds.), Geology and Paleontology of the Lee Creek Mine, North Carolina, III: Smithsonian Contributions to Paleobiology, n. 90, p. 233–365.

OWEN, R., RICHARDSON, C., and KENNEDY, H., 2002. The influence of shell growth rate on striae deposition in the scallop *Pecten maximus*: Journal of the Marine Biological Association of the United Kingdom, v. 82, p. 621–623, doi: 10.1017/S0025315402005969.

PETUCH, E.J., 1982, Notes on the molluscan paleontology of the Pinecrest Beds at Sarasota, Florida, with the description of *Pyruella*, a stratigraphically important new genus (Gastropoda, Melongenidae): Proceedings of the Academy of Natural Sciences of Philadelphia, v. 134, p. 12–30.

PETUCH, E.J. and ROBERTS, C.E., 2007. The Geology of the Everglades and Adjacent Areas: CRC Press, Boca Raton, 212 p.

PURDY, R.W., SCHNEIDER, V.P., APPLEGATE, S.P., MCLELLAN, J.H., MEYER, R.L., and SLAUGHTER, B.H., 2001, The Neogene sharks, rays, and bony fishes from the Lee Creek Mine, Aurora, North Carolina, *in* Ray, C.E. and Bohaska, D.J., eds., Geology and Paleontology of the Lee Creek Mine, North Carolina, III: Smithsonian Contributions to Paleobiology, n. 90, p. 71–202.

RAFFI, S., STANLEY, S.M. and MARASTI, R., 1985, Biogeographic patterns and Plio-Pleistocene extinction of Bivalvia in the Mediterranean and southern North Sea: Paleobiology v. 11, p. 368–388.

RIGGS, S.R., 1984, Paleoceanographic model of Neogene phosphorite deposition, U.S. Atlantic continental margin: Science, v. 223, p. 123–131, doi: 10.1126/science.223.4632.123.

RIGGS, S.R., LEWIS, D.W., SCARBOROUGH, A.K., and SNYDER, S.W., 1982, Cyclic deposition of Neogene phosphorites in the Aurora area, North Carolina, and their possible relationship to global sea-level fluctuations: Southeastern Geology, v. 23, p. 189–203.

RIGGS, S., SNYDER, S., AMES, D., and STILLE, P., 2000, Chronostratigraphy of Upper Cenozoic phosphorites on the North Carolina continental margin and the oceanographic implications for phosphogenesis, *in* Glenn, C.R, Prévôt-Lucas, L., and Lucas, J., eds., Marine Authigenesis: From Global to Microbial: Society of Economic Paleontologists and Mineralogists, Special Publication, n. 66, p. 369–385.

ROULIER, L.M. and QUINN, T.M., 1995, Seasonal-scale to decadal-scale climatic variability in southwest Florida during the Middle Pliocene—inferences from a coralline stable-isotope record: Paleoceanography, v.10, p. 429–443, doi: 10.1029/95PA00374.

SAUPE, E.E., HENDRICKS, J.R., PETERSON, A.T., and LIEBERMAN, B.S., 2014a, Climate change and marine molluscs of the western North Atlantic: future prospects and perils: Journal of Biogeography, v. 41, p. 1352–1366, doi: 10.1111/jbi.12289.

SAUPE, E.E., HENDRICKS, J.R., PORTELL, R.W., DOWSETT, H.J., HAYWOOD, A., HUNTER, S.J., and LIEBERMAN, B.S., 2014b, Macroevolutionary consequences of profound climate change on niche evolution in marine molluscs over the past three million years: Proceedings of the Royal Society, Series B, v. 281, 2014995, 778 KB, doi: 10.1098/rspb.2014.1995.

SIME, J.A. and KELLEY, P.H., 2016, Common mollusk genera indicate interactions with their predators were ecologically stable across the Plio-Pleistocene extinction: Palaeogeography, Palaeoclimatology, Palaeoecology, v. 463, p. 216–229, doi: 10.1016/j.palaeo.2016.10.012.

SMITH, J.T. and JACKSON, J.B.C., 2009, Ecology of extreme faunal turnover of tropical American scallops: Paleobiology, v. 35, p. 77-93, doi: 10.1666/07054.1.

SMITH, J.T, NAKANISHI, N., and JACKSON, J.B.C. 2003. Late Neogene divergence in life span of scallop larvae across the Isthmus of Panama: Geological Society of America, Abstracts with Programs, v. 35(6), p.318.

SNYDER, S.W., HINE, A.C., and RIGGS, S.R., 1990, The seismic stratigraphic record of shifting Gulf Stream flow paths in response to Miocene glacio-eustacy: implications for phosphogenesis along the North Carolina continental margin, *in* Burnett, W.C., and Riggs, S.R., eds., Genesis of Neogene to Recent Phosphorites, Volume 3, Phosphate Deposits of the World: Cambridge University Press, Cambridge, UK, p. 396–423.

STANLEY, S.M., 1970, Relation of Shell Form to Life Habits in the Bivalvia (Mollusca): Geological Society of America (Memoir 125), Boulder, 296 p.

STANLEY, S.M., 1986, Anatomy of a regional mass extinction: Plio-Pleistocene decimation of the Western Atlantic bivalve fauna: PALAIOS, v. 1, p. 17–36.

STANLEY, S.M. and CAMPBELL, L.D., 1981, Neogene mass extinction of western Atlantic molluscs: Nature, v. 293, p. 457–459, doi: 10.1038/293457a0.

STANLEY, S.M. and RUDDIMAN, W.F., 1995. Neogene ice age in the North Atlantic region: climatic changes, biotic effects, and forcing factors, *in* Knoll, A.H. and Stanley, S.M. (eds.), Effects of Past Global Change on Life: National Academy Press, Washington, DC, p. 118–133.

STORER, R.W., 2001. A new Pliocene grebe from the Lee Creek deposits, *in* Ray, C.E. and Bohaska, D.J. (eds.), Geology and Paleontology of the Lee Creek Mine, North Carolina, III: Smithsonian Contributions to Paleobiology, n. 90, p. 227–231.

TAO, K. and GROSSMAN, E.L., 2010, Origin of high productivity in the Pliocene of the Florida Platform: Evidence from stable isotopes and trace elements: PALAIOS, v. 25, p. 796–806, doi: 10.2110/palo.2010.p10-058r.

THÉBAULT, J., CHAUVAUD, L., CLAVIER, J., FICHEZ, R., and MORIZE, E., 2006, Evidence of a 2-day periodicity of striae formation in the tropical scallop *Comptopallium radula* using calcein marking: Marine Biology, v. 149, p. 257-267, doi: 10.1007/s00227-005-0198-8.

THÉBAULT, J. and CHAUVAUD, L., 2013, Li/Ca enrichments in great scallop shells (*Pecten maximus*) and their relationship with phytoplankton blooms: Palaeogeography, Palaeoclimatology, Palaeoecology, v. 373, p. 108–122, doi: 10.1016/j.palaeo.2011.12.014.

THOMPSON, R.J. and MACDONALD, B.A., 1991, Physiological integrations and energy partitioning, *in* Shumway, S.E. (ed.), Scallops: Biology, Ecology and Aquaculture. Developments in Aquaculture and Fisheries Science 21: Elsevier, Amsterdam, The Netherlands and New York, p. 347–376.

TILMAN, D., MAY, R.M., LEHMAN, C.L., and NOWAK, M.A., 1994, Habitat destruction and the extinction debt: Nature, v. 371, p. 65-66, doi: 10.1038/371065a0.

TODD, J.A., JACKSON, J.B.C., JOHNSON, K.G., FORTUNATO, H.M., HEITZ, A., ALVAREZ M., and JUNG, P., 2002, The ecology of extinction: molluscan feeding and faunal turnover in the Caribbean Neogene: Proceedings of the Royal Society, Series B, v. 269, p. 571–577, doi: 10.1098/rspb.2001.1923.

VALENTINE, A., JOHNSON, A.L.A., LENG, M.J., SLOANE, H.J., and BALSON, P.S., 2011, Isotopic evidence of cool winter conditions in the mid-Piacenzian (Pliocene) of the southern North Sea Basin: Palaeogeography, Palaeoclimatology, Palaeoecology, v. 309, p. 9–16, doi: 10.1016/j.palaeo.2011.05.015.

VELARDE, A.A., FLYE-SAINTE-MARIE, J., MENDO, J., and JEAN, F., 2015, Sclerochronological records and daily microgrowth of the Peruvian scallop (*Argopecten purpuratus*, Lamarck, 1819) related to environmental conditions in Paracas Bay, Pisco, Peru: Journal of Sea Research, v. 99, p. 1–8, doi: 10.1016/j.seares.2015.01.002.

VIGNOLS, R.M., VALENTINE, A.M., FINLAYSON, A.G., HARPER, E.M., SCHÖNE, B.R., LENG, M.J., SLOANE, H.J., and JOHNSON, A.L.A., 2018, Marine climate and hydrography of the Coralline Crag (early Pliocene, UK): isotopic evidence from 16 benthic invertebrate taxa. Chemical Geology, v. xx, p. xxx–xxx, doi: 10.1016/j.chemgeo.2018.05.034.

WALLER, T.R., 1969, The evolution of the *Argopecten gibbus* stock (Mollusca: Bivalvia) with emphasis on the Tertiary and Quaternary species of eastern North America: The Palaeontological Society, Memoir 3, 125 p. (Journal of Paleontology, v. 43, Supplement)

WALLER, T.R., 1978, Morphology, morphoclines and a new classification of the Pteriomorphia (Mollusca. Bivalvia), *in* Yonge, C.M. and Thompson, T.E., (eds.), Evolutionary Systematics of Bivalve Molluscs: Philosophical Transactions of the Royal Society of London, Series B, v. 284, p. 345–365.

WALLER, T.R., 2018, Systematics and biostratigraphy of *Chesapecten* and *Carolinapecten* (Mollusca: Bivalvia: Pectinidae) in the upper Miocene and Pliocene "lower Tamiami Formation" of southwestern Florida: Bulletin of the Florida Museum of Natural History, v. 56, p. 1-47.

WALLISER, E.O., SCHÖNE, B.R., TÜTKEN, T., ZIRKEL, J., GRIMM, K.I., and PROSS, J., 2015, The bivalve *Glycymeris planicostalis* as a high-resolution paleoclimate archive for the Rupelian (Early Oligocene) of central Europe. Climate of the Past, v. 11, p. 653–668, doi: 10.5194/cp-11-653-2015.

WARD, L.W., 2008, Synthesis of palaeontological and stratigraphic investigations at the Lee Creek Mine, Aurora, N.C. (1958–2007), *in* Ray, C.E., Bohaska, D.J., Koretsky, I.A., Ward, L.W., and Barnes, L.G. (eds.), Geology and Paleontology of the Lee Creek Mine, North Carolina, IV: Virginia Museum of Natural History Special Publication, n. 14, p. 325–436 (including Addendum by Bohaska, D.J.).

WARD, L.W. and BLACKWELDER, B.W., 1980, Stratigraphic revision of upper Miocene and lower Pliocene beds of the Chesapeake Group, Middle Atlantic Coastal Plain: U.S. Geological Survey Bulletin, n. 1482-D, p. 1–61.

WARD, L.W. and BLACKWELDER, B.W., 1987, Late Pliocene and early Pleistocene Mollusca from the James City and Chowan River formations at the Lee Creek Mine, *in* Ray, C.E. (ed.), Geology and Paleontology of the Lee Creek Mine, North Carolina, II: Smithsonian Contributions to Paleobiology, n. 61, p. 113–283.

WARD, L.W., BAILEY R.H., and CARTER, J.G., 1991, Pliocene and early Pleistocene stratigraphy, depositional history, and molluscan paleobiogeography of the Coastal Plain, *in* Horton, J.W., Jr. and Zullo, V.A., eds., The Geology of the Carolinas: University of Tennessee Press, Knoxville, Tennessee, p. 274–289.

WESTGATE, J.W. and WHITMORE, F.C. Jr., 2002, *Balaena ricei*, a new species of bowhead whale from the Yorktown Formation (Pliocene) of Hampton, Virginia, *in* Emry, R.J. (ed.), Cenozoic Mammals of Land and Sea: Tributes to the Career of Clayton E. Ray: Smithsonian Contributions to Paleobiology, n. 93, p. 295–312.

WHITEHEAD, D.R., 1983, Pollen analysis of the peat member from the Lee Creek Mine: *in* Ray, C.E. (ed.), Geology and Paleontology of the Lee Creek Mine, North Carolina, I: Smithsonian Contributions to Paleobiology, n. 53, p. 265–268.

WHITMORE, F.C. JR and BARNES, L.G., 2008, The Herpetocetinae, a new subfamily of extinct baleen whales (Mammalia, Cetacea, Cetotheriidae), *in* Ray, C.E., Bohaska, D.J., Koretsky, I.A., Ward, L.W., and Barnes, L.G. (eds.), Geology and Paleontology of the Lee Creek Mine, North Carolina, IV: Virginia Museum of Natural History Special Publication, n. 14, p. 141–180.

WHITMORE, F.C. JR and KALTENBACH, J.A., 2008, Neogene Cetacea of the Lee Creek phosphate mine, *in* Ray, C.E., Bohaska, D.J., Koretsky, I.A., Ward, L.W., and Barnes, L.G. (eds.), Geology and Paleontology of the Lee Creek Mine, North Carolina, IV: Virginia Museum of Natural History Special Publication, n. 14, p. 181–269.

WILLIAMS, M.J. and DREDGE, M.C.L., 1981, Growth of the saucer scallop *Amusium japonicum balloti* Habe in central eastern Queensland: Australian Journal of Marine and Freshwater Research, v. 32, p. 657–666.

WILLIAMS, M., HAYWOOD, A.M., HARPER, E.M., JOHNSON, A.L.A., KNOWLES, T., LENG, M.J., LUNT, D.J., OKAMURA, B., TAYLOR, P.D., and ZALAZIEWICZ, J., 2009, Pliocene climate and seasonality in North Atlantic shelf seas: Philosophical Transactions of the Royal Society, Series A, v. 367, p. 85–108, doi: 10.1098/rsta.2008.0224.

WINKELSTERN, I., SURGE, D., and HUDLEY, J.W., 2013, Multiproxy sclerochronological evidence for Plio-Pleistocene regional warmth: United States Mid-Atlantic Coastal Plain: PALAIOS, v. 28, p. 649–660, doi: 10.2110/palo.2013.p13-010r.

WINKELSTERN, I. Z., ROWE, M.P., LOHMANN, K.C., DEFLIESE, W.F., PETERSEN, S.V., and BREWER, A.W., 2017. Meltwater pulse recorded in Last Interglacial mollusk shells from Bermuda: Paleoceanography, v. 32, 10.1002/2016PA003014, 1.1 MB, doi: 10.1002/2016PA003014. Checked November 2018.

FIGURE CAPTIONS

FIG. 1.—Specimens of *Carolinapecten eboreus* and an example of the extant scallop *Aequipecten opercularis* from the Pliocene of the UK, showing overall morphology, microgrowth increments, and the positions of growth breaks and certain δ^{18}O values. **A**) *C. eboreus* LPLI-GCP 5 (right valve; Very Fast growth rate). **B**) *C. eboreus* LPLI-GCP 3 (left valve; Fast growth rate). **C**) *C. eboreus* EPLE-MACP 1 (right valve; Medium growth rate). **D**) *A. opercularis* UD 52795 (right valve). **E**) Enlargement of area indicated in B. **F**)

Enlargement of area indicated in C. **G**) Enlargement of area indicated in D. Scale bars (vertical: A−D; horizontal: E–G) = 10 mm. S1/2 and W1/2 in A–D mark the positions of extreme summer and winter $\delta^{18}O$ values, respectively ($\delta^{18}O$ data for D in Johnson et al. 2009, fig. 8A). Other symbols in A–C signify the points between which the largest whole-year increments (green circles) and largest half-year increments (purple semicircles; superimposed on green circle where whole- and half-year increment boundaries coincide) were measured on the basis of $\delta^{18}O$ profiles (Figs. 6E, 6C and 8D, respectively), and the positions of major (filled blue triangles) and moderate (open blue triangle) growth breaks (see also F for the form of major growth breaks). Since the shell in C is incomplete, measurements were mathematically adjusted (see text) to correspond to measurements along the mid-line (anatomical height). The size of the microgrowth increments (bounded by commarginal lamellae) in F is similar to those in G (*A. opercularis*), and in other scallop species (e.g., Owen et al. 2002). Note the very much larger microgrowth increments in E. Although these are at the high end of the size-range in *C. eboreus*, microgrowth increments only slightly smaller are typical of the species (Table 2).

FIG. 2.—Chronostratigraphic position (age in Ma) of EPLI (brown), LPLI (pink) and EPLE (light blue) *C. eboreus* specimens, with corresponding museum accession numbers and/or specimen codes of Krantz (1990) and Jones and Allmon (1995). Broad age estimates for the source units are signified by thin lines; more precise (but not necessarily accurate) estimates by thick lines (double thickness where two estimates coincide). In some cases there were imprecise and/or alternative source units, signified by dashed lines. Source units indicated in the text; details, together with evidence of age, in Supplementary Data File 1.

FIG. 3.—Geographic provenance of *C. eboreus* specimens (see text for names of locations).

FIG. 4.—Temperature and production characteristics of time-space divisions recognised herein, based on earlier studies (see text).

FIG. 5.—Data for $\delta^{18}O$, $\delta^{13}C$, microgrowth-increment height and growth-break position from EPLI-GCP and EPLI-MACP specimens of *C. eboreus*. **A**) EPLI-GCP 1. **B**) EPLI-MACP 1. **C**) EPLI-GCP 2. **D**) EPLI-MACP 2. Isotope data represented by crosses = replicate analyses for a given position, the mean or most reasonable single value being used in the relevant profile (line). Dashed line for microgrowth-increment height = raw data; continuous line = 5-point averages. Filled and open triangles (blue) = major and moderate growth breaks, respectively. Semicircles (purple) and circles (green) = $\delta^{18}O$ values defining the largest half- and whole-year increments, respectively (semicircles superimposed on circles where boundaries of half- and whole-year increments coincide). S1/2 and W1/2 = summers and winters, respectively, as identified from the $\delta^{18}O$ profiles. Isotopic axis reversed so that lower values of $\delta^{18}O$ (representative of higher temperatures) plot towards the top.

FIG. 6.—Data for $\delta^{18}O$, $\delta^{13}C$, microgrowth-increment height and growth-break position from LPLI-GCP specimens of *C. eboreus*. **A**) LPLI-GCP 1. **B**) LPLI-GCP 2. **C**) LPLI-GCP 3. **D**) LPLI-GCP 4. **E**) LPLI-GCP 5. **F**) LPLI-GCP 6. Symbols and format explained in Figure 5, with the exception of stars (marking aberrant early ontogenetic $\delta^{18}O$ values, thought to reflect diagenetic alteration; see text).

FIG. 7.—Data for $\delta^{18}O$, $\delta^{13}C$, microgrowth-increment height and growth-break position from LPLI-MACP specimens of *C. eboreus*. **A**) LPLI-MACP 1. **B**) LPLI-MACP 2. **C**) LPLI-

MACP 3. **D**) LPLI-MACP 4. **E**) LPLI-MACP. **F**) LPLI-MACP 6. Symbols and format explained in Figures 5 and 6.

FIG. 8.—Data for δ^{18}O, δ^{13}C, microgrowth-increment height and growth-break position from EPLE-GCP and EPLE-MACP specimens of *C. eboreus*. **A**) EPLE-GCP 1. **B**) EPLE-MACP 1. **C**) EPLE-GCP 2. **D**) EPLE-MACP 2. Symbols and format explained in Figure 5.

FIG. 9.—Number and mean size (height) of microgrowth increments versus size (height) of the largest half- and whole-year increment in *C. eboreus* specimens (data from Table 2). **A**) Number of microgrowth increments per half-year increment in specimens whose δ^{18}O profiles have summer/winter inflections precisely defining the largest half-year increment. **B**) as A but for mean size of microgrowth increments. **C**) As A but for whole-year increments. **D**) As B but for whole-year increments. **E**) As A but with the addition of specimens whose δ^{18}O profiles have insufficient inflections to precisely define the largest half-year increment, providing only minimum estimates. **F**) As E but for mean size of microgrowth increments. **G**) As E but for whole-year increments. **H**) As F but for whole-year increments.

FIG. 10.—Growth rate of shells in relation to δ^{18}O-derived summer and winter temperatures (referred to the categories identified in Fig. 4) and primary production (inferred from the associated biota). Second entries in smaller typeface represent alternative interpretations of seasonal temperature (where the δ^{18}O profile was of insufficient length to provide conclusive evidence) and/or production (from δ^{13}C evidence); see text for further information. The 'flat' δ^{18}O profile from LPLI-GCP 3 (Fig. 6C) is interpreted as a high temperature winter record (see text); in the absence of a summer record, classification in terms of seasonal temperature

can only be partial, as indicated by the two entries in parentheses and the same (standard) typeface, signifying equal probability.

TABLE CAPTIONS

TABLE 1.—Winter minimum and summer maximum temperatures calculated from the shell δ^{18}O of various bivalve mollusk genera from 'early Pliocene' (EPLI), 'late Pliocene' (LPLI) and early Pleistocene (EPLE) stratigraphic units of the Middle Atlantic Coastal Plain (see Supplementary Data File 1 for evidence of age). Superscripts indicate the source of the δ^{18}O data: a = Krantz (1990); b = Goewert and Surge (2008); c = Winkelstern et al. (2013); d = Johnson et al. (2017). The figures given are based on the largest maximum (winter) and smallest minimum (summer) δ^{18}O values from individual profiles; the corresponding individual seasonal temperatures were either those supplied by the original authors (Winkelstern et al. 2013; Johnson et al. 2017) or values recalculated as specified in Johnson et al. (2017) or herein (see text). Water δ^{18}O values of +0.70‰ (EPLI), +1.10‰ (LPLI) and 0.00‰ (EPLE) were used.

TABLE 2.—Size (height) of the largest half- and whole-year increments in specimens of *C. eboreus* (as measured from δ^{18}O profiles), together with the number and mean size (height) of microgrowth increments in these half- and whole-year increments (where determined). Key to superscripts (sources of shell δ^{18}O data): a = this study; b = Jones and Allmon (1995, fig. 10); c = Krantz (1990, figs. 4b, 5b, 6–8).

TABLE 3.—Individual and divisional mean winter and summer temperatures calculated using the largest maximum (winter) and smallest minimum (summer) values of shell δ^{18}O from

each specimen (see Supplementary Data File 4), in combination with the preferred value of water $\delta^{18}O$ for the division concerned (see text) and an arbitrary common value (+0.7‰). Key to superscripts (sources of shell $\delta^{18}O$ data): a = this study; b = Jones and Allmon (1995, fig. 10); c = Krantz (1990, tables 3–5).

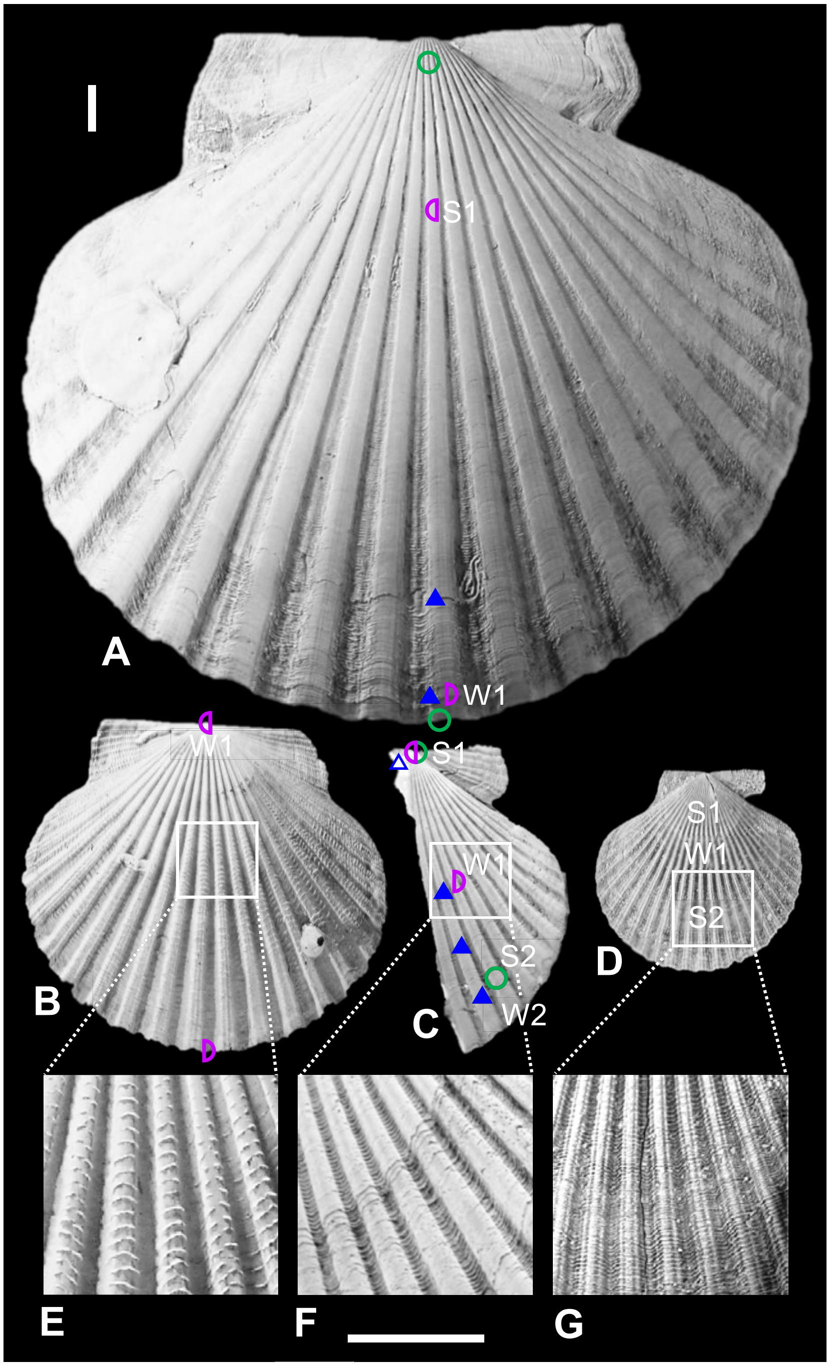

FIGURE 1

FIGURE 2

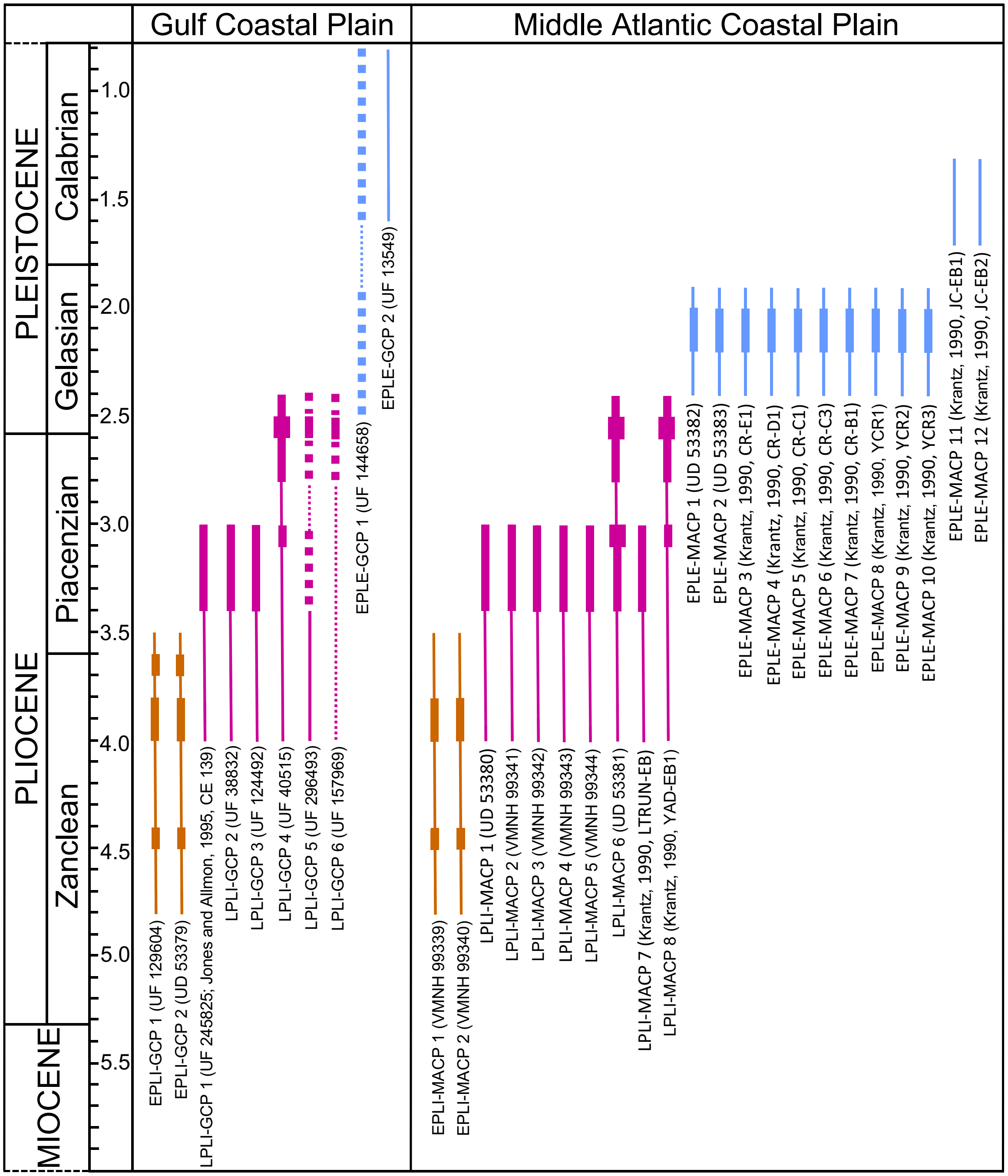
Gulf Coastal Plain
Middle Atlantic Coastal Plain
PLEISTOCENE
PLIOCENE
MIOCENE
Calabrian
Gelasian
Piacenzian
Zanclean
1.0
1.5
2.0
2.5
3.0
3.5
4.0
4.5
5.0
5.5
EPLI-GCP 1 (UF 129604)
EPLI-GCP 2 (UD 53379)
LPLI-GCP 1 (UF 245825; Jones and Allmon, 1995, CE 139)
LPLI-GCP 2 (UF 38832)
LPLI-GCP 3 (UF 124492)
LPLI-GCP 4 (UF 40515)
LPLI-GCP 5 (UF 296493)
LPLI-GCP 6 (UF 157969)
EPLE-GCP 1 (UF 144658)
EPLE-GCP 2 (UF 13549)
EPLI-MACP 1 (VMNH 99339)
EPLI-MACP 2 (VMNH 99340)
LPLI-MACP 1 (UD 53380)
LPLI-MACP 2 (VMNH 99341)
LPLI-MACP 3 (VMNH 99342)
LPLI-MACP 4 (VMNH 99343)
LPLI-MACP 5 (VMNH 99344)
LPLI-MACP 6 (UD 53381)
LPLI-MACP 7 (Krantz, 1990, LTRUN-EB)
LPLI-MACP 8 (Krantz, 1990, YAD-EB1)
EPLE-MACP 1 (UD 53382)
EPLE-MACP 2 (UD 53383)
EPLE-MACP 3 (Krantz, 1990, CR-E1)
EPLE-MACP 4 (Krantz, 1990, CR-D1)
EPLE-MACP 5 (Krantz, 1990, CR-C1)
EPLE-MACP 6 (Krantz, 1990, CR-C3)
EPLE-MACP 7 (Krantz, 1990, CR-B1)
EPLE-MACP 8 (Krantz, 1990, YCR1)
EPLE-MACP 9 (Krantz, 1990, YCR2)
EPLE-MACP 10 (Krantz, 1990, YCR3)
EPLE-MACP 11 (Krantz, 1990, JC-EB1)
EPLE-MACP 12 (Krantz, 1990, JC-EB2)

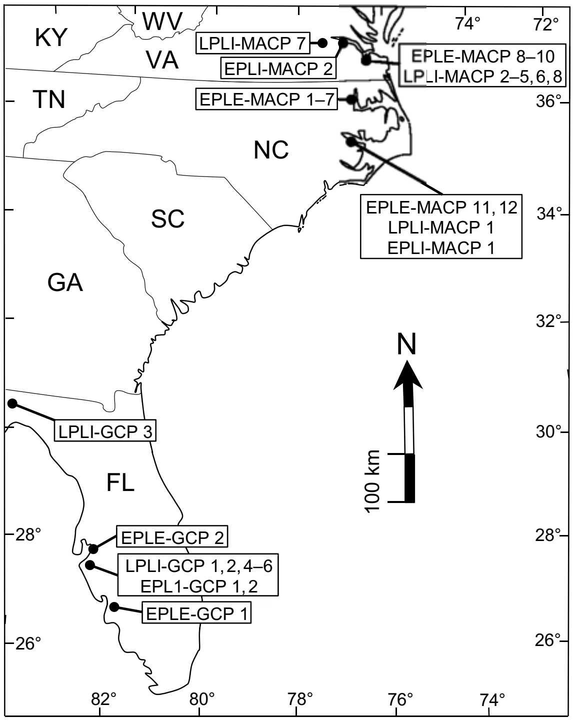
KY
WV
VA
TN
NC
SC
GA
FL
74°
72°
LPLI-MACP 7
EPLI-MACP 2
EPLE-MACP 8–10
LPLI-MACP 2–5, 6, 8
EPLE-MACP 1–7
36°
EPLE-MACP 11, 12
LPLI-MACP 1
EPLI-MACP 1
34°
32°
N
LPLI-GCP 3
30°
100 km
28°
EPLE-GCP 2
28°
LPLI-GCP 1, 2, 4–6
EPL1-GCP 1, 2
EPLE-GCP 1
26°
26°
82°
80°
78°
76°
74°

FIGURE 4

Temperature	Primary production	
	‘Average’	High
High summer (HS): ≥ 24 °C High winter (HW): ≥ 11.5 °C	LPLI-MACP	LPLI-GCP
High summer (HS): ≥ 24 °C Low winter (LW): < 11.5 °C		
Low summer (LS): < 24 °C High winter (HW): ≥ 11.5 °C	EPLE-GCP	EPLI-GCP
Low summer (LS): < 24 °C Low winter (LW): < 11.5 °C	EPLE-MACP	EPLI-MACP

FIGURE 5

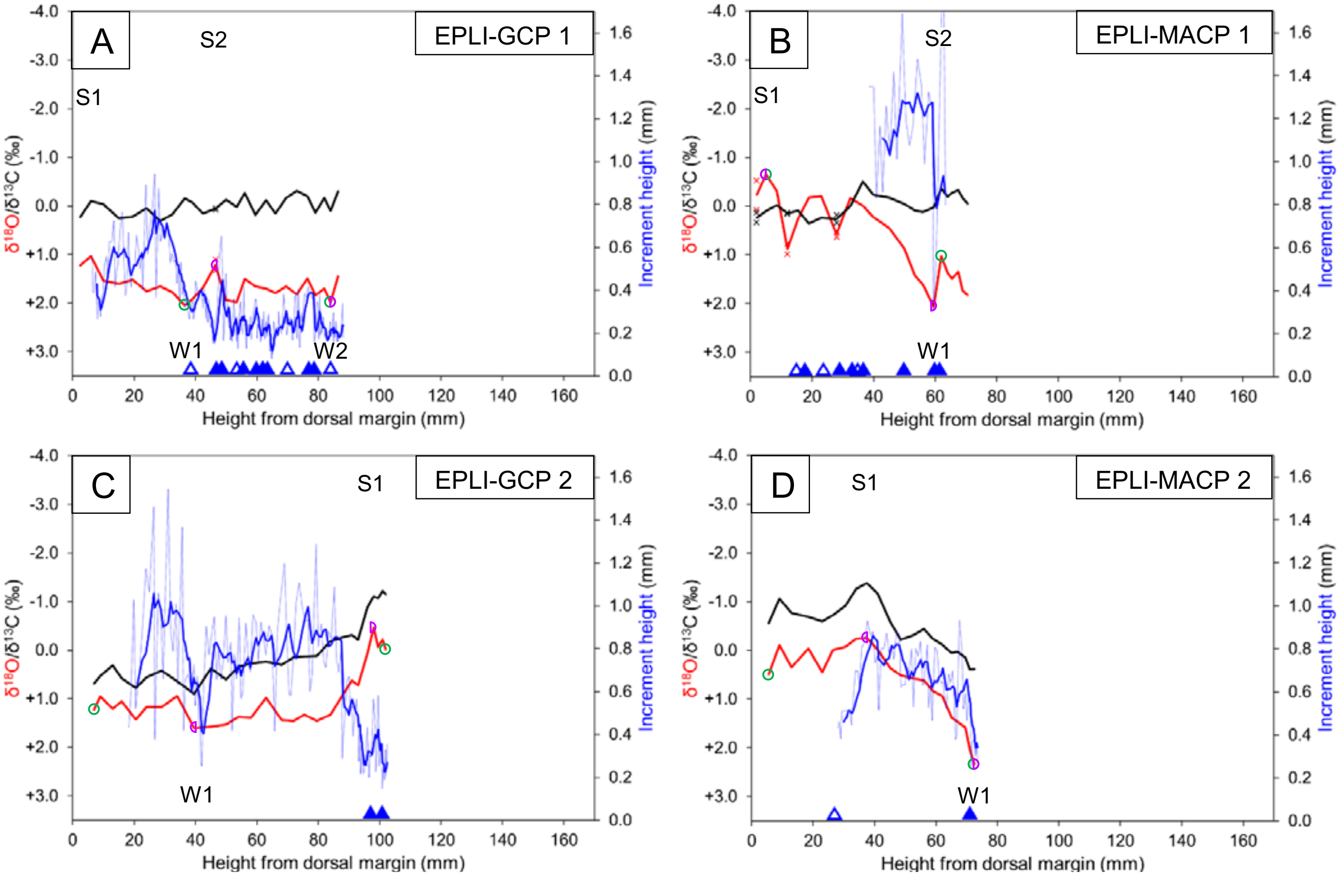
A
EPLI-GCP 1
S1
S2
W1
W2
B
EPLI-MACP 1
S1
S2
W1
C
EPLI-GCP 2
S1
W1
D
EPLI-MACP 2
S1
W1
$\delta^{18}O/\delta^{13}C$ (‰)
Increment height (mm)
Height from dorsal margin (mm)
-4.0
-3.0
-2.0
-1.0
0.0
+1.0
+2.0
+3.0
0
20
40
60
80
100
120
140
160
0.0
0.2
0.4
0.6
0.8
1.0
1.2
1.4
1.6

FIGURE 6

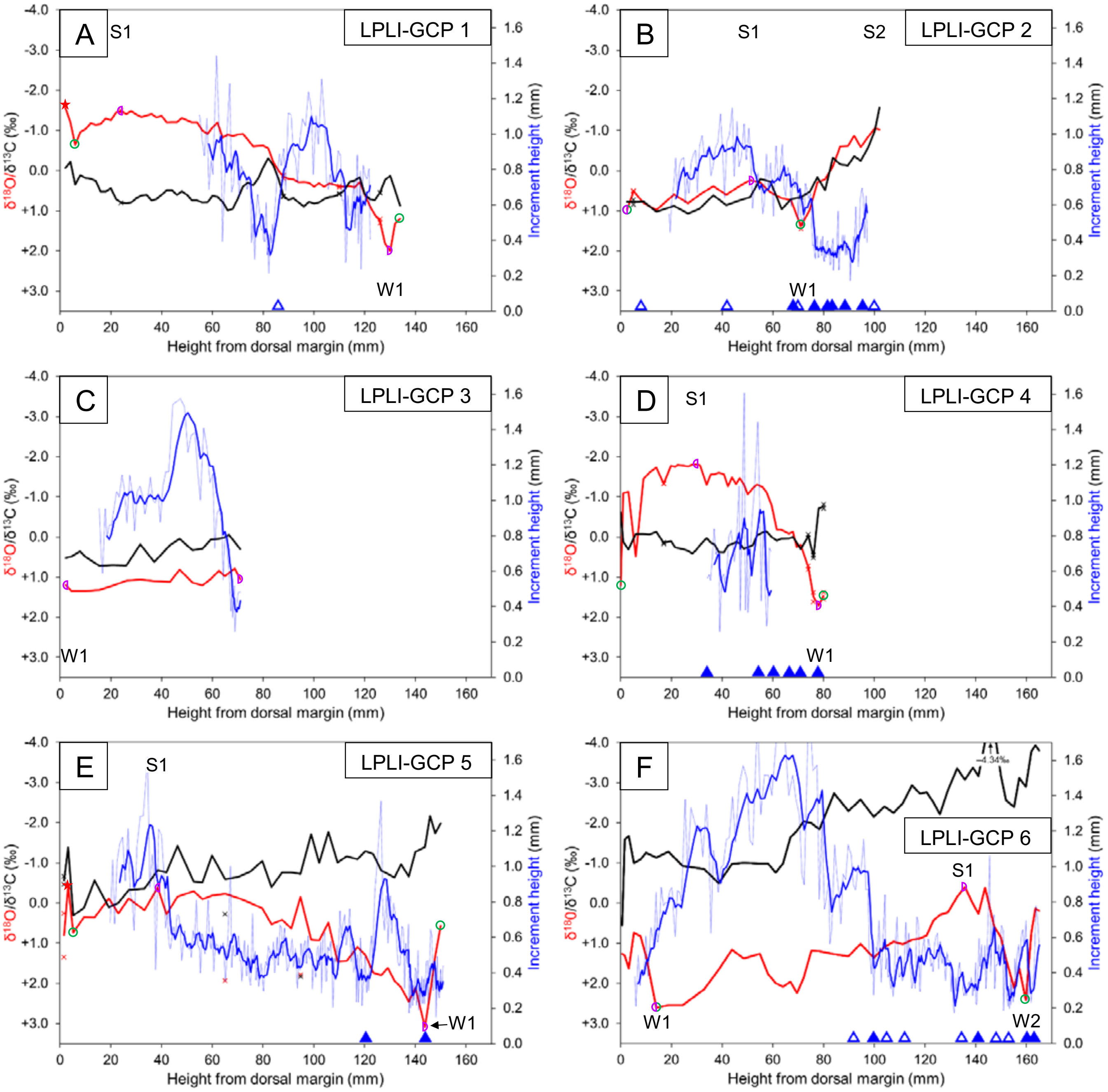
A
LPLI-GCP 1
S1
W1
B
LPLI-GCP 2
S1
S2
W1
C
LPLI-GCP 3
W1
D
LPLI-GCP 4
S1
W1
E
LPLI-GCP 5
S1
←W1
F
LPLI-GCP 6
S1
W1
W2
-4.34‰
δ¹⁸O/δ¹³C (‰)
Increment height (mm)
Height from dorsal margin (mm)
-4.0
-3.0
-2.0
-1.0
0.0
+1.0
+2.0
+3.0
1.6
1.4
1.2
1.0
0.8
0.6
0.4
0.2
0.0
0
20
40
60
80
100
120
140
160

FIGURE 7

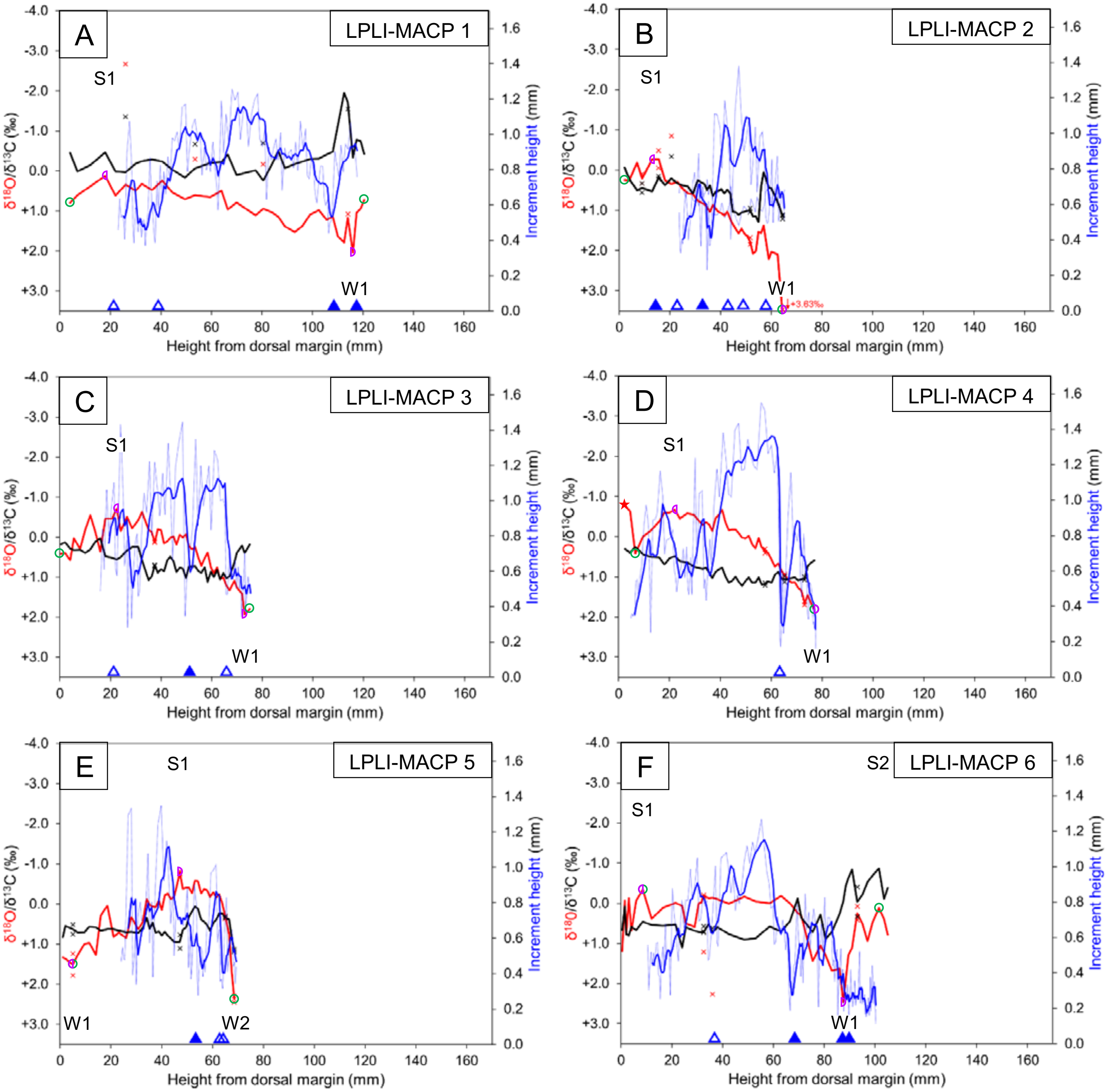
A
LPLI-MACP 1
S1
W1
B
LPLI-MACP 2
S1
W1
+3.63‰
C
LPLI-MACP 3
S1
W1
D
LPLI-MACP 4
S1
W1
E
LPLI-MACP 5
S1
W1
W2
F
LPLI-MACP 6
S1
S2
W1
δ18O/δ13C (‰)
-4.0
-3.0
-2.0
-1.0
0.0
+1.0
+2.0
+3.0
Increment height (mm)
1.6
1.4
1.2
1.0
0.8
0.6
0.4
0.2
0.0
Height from dorsal margin (mm)
0
20
40
60
80
100
120
140
160

FIGURE 8

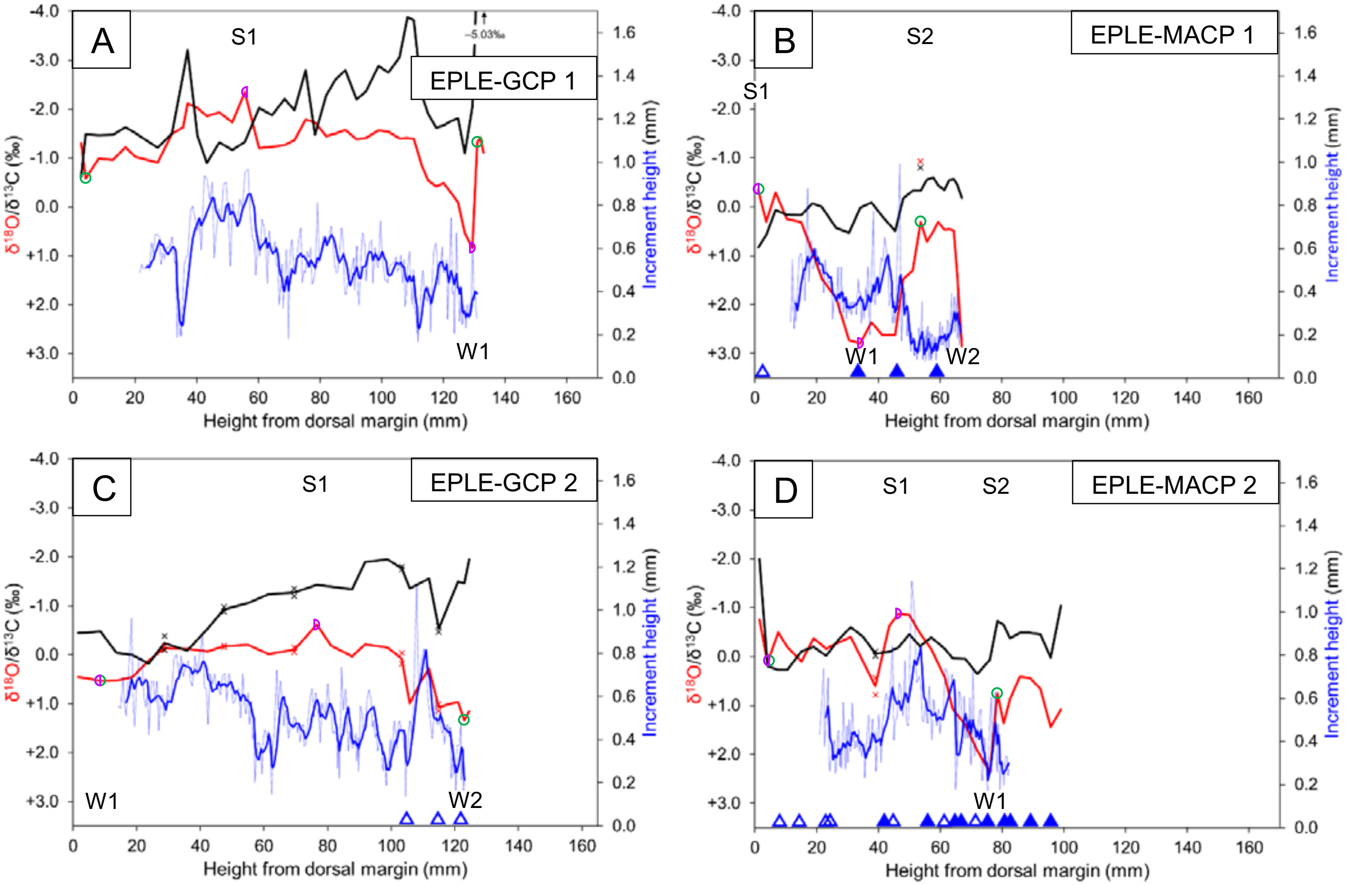
A
EPLE-GCP 1
S1
W1
-5.03‰
B
EPLE-MACP 1
S1
S2
W1
W2
C
EPLE-GCP 2
S1
W1
W2
D
EPLE-MACP 2
S1
S2
W1
δ18O/δ13C (‰)
Increment height (mm)
Height from dorsal margin (mm)
-4.0
-3.0
-2.0
-1.0
0.0
+1.0
+2.0
+3.0
0.0
0.2
0.4
0.6
0.8
1.0
1.2
1.4
1.6
0
20
40
60
80
100
120
140
160

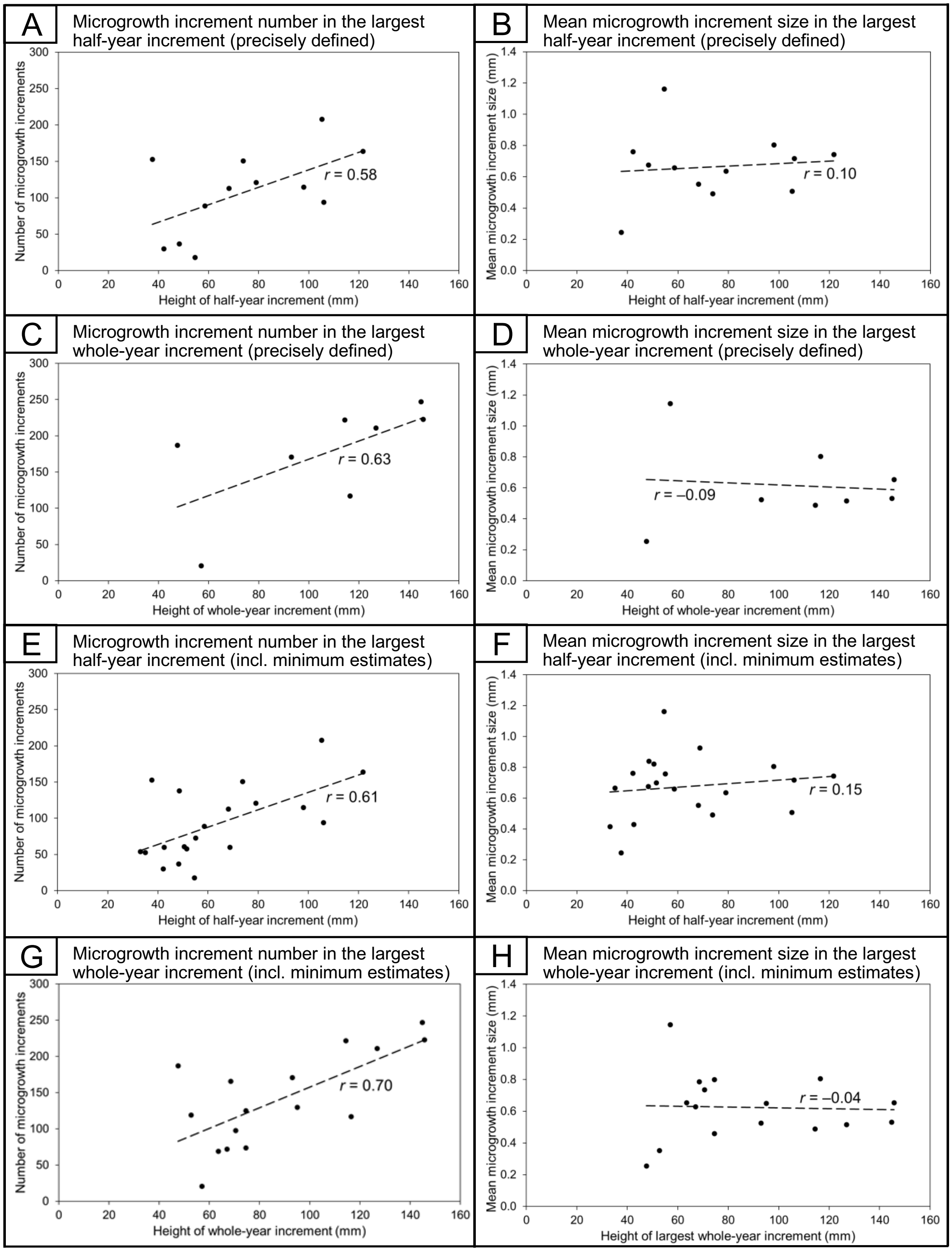
A
Microgrowth increment number in the largest half-year increment (precisely defined)
Number of microgrowth increments
Height of half-year increment (mm)
r = 0.58
B
Mean microgrowth increment size in the largest half-year increment (precisely defined)
Mean microgrowth increment size (mm)
Height of half-year increment (mm)
r = 0.10
C
Microgrowth increment number in the largest whole-year increment (precisely defined)
Number of microgrowth increments
Height of whole-year increment (mm)
r = 0.63
D
Mean microgrowth increment size in the largest whole-year increment (precisely defined)
Mean microgrowth increment size (mm)
Height of whole-year increment (mm)
r = –0.09
E
Microgrowth increment number in the largest half-year increment (incl. minimum estimates)
Number of microgrowth increments
Height of half-year increment (mm)
r = 0.61
F
Mean microgrowth increment size in the largest half-year increment (incl. minimum estimates)
Mean microgrowth increment size (mm)
Height of half-year increment (mm)
r = 0.15
G
Microgrowth increment number in the largest whole-year increment (incl. minimum estimates)
Number of microgrowth increments
Height of whole-year increment (mm)
r = 0.70
H
Mean microgrowth increment size in the largest whole-year increment (incl. minimum estimates)
Mean microgrowth increment size (mm)
Height of largest whole-year increment (mm)
r = –0.04
0 50 100 150 200 250 300
0.0 0.2 0.4 0.6 0.8 1.0 1.2 1.4
0 20 40 60 80 100 120 140 160

FIGURE 9

Temperature	‘Average’ primary production				High primary production			
	Growth rate				Growth rate			
	Slow ½-yr: < 30 mm 1-yr: < 60 mm	Medium ½-yr: > 30 mm 1-yr: > 60 mm	Fast ½-yr: > 60 mm 1-yr: > 90 mm	Very Fast ½-yr: > 90 mm 1-yr: > 120 mm	Slow ½-yr: < 30 mm 1-yr: < 60 mm	Medium ½-yr: > 30 mm 1-yr: > 60 mm	Fast ½-yr: > 60 mm 1-yr: > 90 mm	Very Fast ½-yr: > 90 mm 1-yr: > 120 mm
HS/HW	LPLI-MACP 7	LPLI-MACP 3 LPLI-MACP 8		EPLE-GCP 1		LPLI-GCP 2 LPLI-GCP 4	(LPLI-GCP 3)	EPLE-GCP 1
HS/LW		LPLI-MACP 5		EPLE-GCP 1		LPLI-GCP 4		LPLI-GCP 1
LS/HW	LPLI-MACP 7	LPLI-MACP 3 LPLI-MACP 4	LPLI-MACP 1				EPLI-GCP 2 (LPLI-GCP 3)	
LS/LW	EPLE-MACP 4 EPLE-MACP 5 EPLE-MACP 6 EPLE-MACP 8 EPLE-MACP 9 EPLE-MACP 10 EPLE-MACP 11 EPLE-MACP 12	LPLI-MACP 2 LPLI-MACP 3 LPLI-MACP-4 LPLI-MACP 5 EPLE-MACP 1 EPLE-MACP 2 EPLE-MACP 3 EPLE-MACP 7	LPLI-MACP 1 LPLI-MACP 6 EPLE-GCP 2			EPLI-GCP 1 EPLI-MACP 1 EPLI-MACP 2	EPLE-GCP 2	LPLI-GCP 5 LPLI-GCP 6

FIGURE 10

TABLE 1

Age	Formation	Member	Genus	Winter minimum temperature (°C)		Summer maximum temperature (°C)	
				Mean value ± 1σ (n)	Singleton value	Mean value ± 1σ (n)	Singleton value
EPLE	James City Fm (lower)		*Carolinapecten*[a]	6.6 ± 0.9 (2)		19.8 ± 0.5 (2)	
	Chowan River Formation		*Carolinapecten*[a]	7.5 ± 1.6 (8)		20.8 ± 1.9 (8)	
			Mercenaria[c]	10.5 ± 0.5 (6)		22.0 ± 2.2 (6)	
LPLI	Yorktown Formation (upper|)	Moore House	*Carolinapecten*[a]		14.5		26.8
			Chesapecten[a, b]	11.5 ± 2.1 (5)		27.7 ± 1.7 (5)	
		Morgarts Beach	*Carolinapecten*[a]		12.5		
		Rushmere	*Mercenaria*[c]	17 ± 1.8 (6)		26.2 ± 1.8 (6)	
			Chesapecten[a]		13.3		29.3
EPLI	Yorktown Formation (lower)	Sunken Meadow	*Chesapecten*[a]	11.4 ± 0.7 (3)		23.0 ± 1.0 (2)	
			Placopecten[d]	8.5 ± 0.9 (8)		17.3 ± 1.2 (8)	

Specimen code and source of δ^{18}O data (a, b, c)	Largest half-year increment (by δ^{18}O)			Largest whole-year increment (by δ^{18}O)		
	Height (mm)	Microgrowth increments		Height (mm)	Microgrowth increments	
		Number	Mean height (mm)		Number	Mean height (mm)
EPLI-GCP 1[a]	37.5	153	0.245	47.5	187	0.255
EPLI-GCP 2[a]	58.5	89	0.659	> 95.0	> 130	0.650
EPLI-MACP 1[a]	54.5	> 18	1.163	57.0	> 21	1.146
EPLI-MACP 2[a]	> 35.0	> 53	0.665	> 67.0	> 72	0.628
LPLI-GCP 1[b]	106.0	> 94	0.718	> 128		
LPLI-GCP 2[a]	> 48.5	> 38	0.841	> 68.5	> 166	0.786
LPLI-GCP 3[a]	> 68.7	> 60	0.926			
LPLI-GCP 4[a]	48.2	> 37	0.676	> 80.0		
LPLI-GCP 5[a]	105.2	208	0.507	144.8	> 247	0.532
LPLI-GCP 6[a]	121.7	164	0.743	145.7	223	0.655
LPLI-MACP 1[a]	98.0	> 115	0.805	116.5	> 117	0.805
LPLI-MACP 2[a]	> 51.5	> 58	0.699	> 62.5		
LPLI-MACP 3[a]	> 50.5	> 61	0.823	> 74.5	> 74	0.799
LPLI-MACP 4[a]	> 55.0	> 73	0.757	> 70.5	> 98	0.735
LPLI-MACP 5[a]	42.1	> 30	0.761	> 63.5	> 69	0.655
LPLI-MACP 6[a]	79.0	121	0.636	93.0	> 171	0.525
LPLI-MACP 7[c]	> 20.0					
LPLI-MACP 8[c]	> 34.0					
EPLE-GCP 1[a]	73.7	151	0.491	126.8	> 211	0.517
EPLE-GCP 2[a]	68.0	> 113	0.553	114.4	> 222	0.489
EPLE-MACP 1[a]	> 33.0	> 54	0.416	> 52.6	> 119	0.353
EPLE-MACP 2[a]	> 42.5	> 60	0.429	> 74.5	> 125	0.460
EPLE-MACP 3[c]	> 30					
EPLE-MACP 4[c]	25.0			42.0		
EPLE-MACP 5[c]	> 29.0			> 46.0		
EPLE-MACP 6[c]	16.0			26.0		
EPLE-MACP 7[c]	> 47.0					
EPLE-MACP 8[c]	25.0			43.0		
EPLE-MACP 9[c]	23.0			40.0		
EPLE-MACP 10[c]	24.0			41.0		
EPLE-MACP 11[c]	25.0			> 45.0		
EPLE-MACP 12[c]	24.0					

TABLE 2

TABLE 3

Specimen/division code; source of shell δ^{18}O data (a, b, c)	Temperature (°C) for the preferred water δ^{18}O		Temperature (°C) for water δ^{18}O = +0.7‰	
	Winter	Summer	Winter	Summer
EPLI-GCP 1[a]	10.7	14.8	9.9	14.0
EPLI-GCP 2[a]	12.5	21.4	11.7	20.5
EPLI-GCP mean	11.6 ± 0.9	18.1 ± 3.3	10.8 ± 0.9	17.3 ± 3.3
EPLI-MACP 1[a]	9.8	21.3	9.8	21.3
EPLI-MACP 2[a]	8.8	19.5	8.8	19.5
EPLI-MACP mean	9.3 ± 0.5	20.4 ± 0.9	9.3 ± 0.5	20.4 ± 0.9
LPLI-GCP 1[b]	11.3	26.8	10.1	25.2
LPLI-GCP 2[a]	13.8	24.7	12.5	23.2
LPLI-GCP 3[a]	14.0		12.7	
LPLI-GCP 4[a]	12.5	28.5	11.2	26.9
LPLI-GCP 5[a]	7.2	21.6	6.1	20.1
LPLI-GCP 6[a]	9.0	21.7	7.8	20.2
LPLI-GCP mean	11.3 ± 2.5	24.7 ± 2.7	10.1 ± 2.4	23.1 ± 2.7
LPLI-MACP 1[a]	11.5	19.6	10.0	17.8
LPLI-MACP 2[a]	5.6	21.4	4.2	19.6
LPLI-MACP 3[a]	12.0	23.5	10.4	21.6
LPLI-MACP 4[a]	12.4	23.3	10.8	21.4
LPLI-MACP 5[a]	10.2	23.8	12.0	21.9
LPLI-MACP 6[a]	9.8	21.7	8.3	19.9
LPLI-MACP 7[c]	12.5	18.8	10.9	17.1
LPLI-MACP 8[c]	14.5	26.8	12.9	24.8
LPLI-MACP mean	11.1 ± 2.5	22.4 ± 2.4	9.9 ± 2.4	20.5 ± 2.3
EPLE-GCP 1[a]	11.9	26.0	14.7	29.5
EPLE-GCP 2[a]	10.0	18.0	12.7	21.2
EPLE-GCP mean	11.0 ± 1.0	22.0 ± 4.0	13.7 ± 1.0	25.4 ± 4.2
EPLE-MACP 1[a]	4.4	16.8	6.9	19.9
EPLE-MACP 2[a]	6.1	19.2	8.7	22.4
EPLE-MACP 3[c]	6.4	17.9	8.9	21.1
EPLE-MACP 4[c]	5.7	17.9	8.2	21.1
EPLE-MACP 5[c]	6.4	19.7	8.9	22.9
EPLE-MACP 6[c]	6.4	22.0	8.9	25.3
EPLE-MACP 7[c]	6.7	22.9	9.3	26.3
EPLE-MACP 8[c]	9.3	22.0	12.1	25.3
EPLE-MACP 9[c]	9.7	21.5	12.5	24.8
EPLE-MACP 10[c]	9.3	22.5	12.1	25.8
EPLE-MACP 11[c]	7.5	20.2	10.1	23.4
EPLE-MACP 12[c]	5.7	19.3	8.2	22.5
EPLE-MACP mean	7.0 ± 1.6	20.2 ± 1.9	9.6 ± 1.7	23.4 ± 2.0